

A relocatable ocean model in support of environmental emergencies

The Costa Concordia emergency case

Michela De Dominicis · Silvia Falchetti · Francesco Trotta ·
Nadia Pinardi · Luca Giacomelli · Ernesto Napolitano · Leopoldo Fazioli ·
Roberto Sorgente · Patrick J. Haley Jr. · Pierre F. J. Lermusiaux ·
Flavio Martins · Michele Cocco

Received: 15 October 2013 / Accepted: 12 February 2014
© The Author(s) 2014. This article is published with open access at Springerlink.com

Abstract During the Costa Concordia emergency case, regional, subregional, and relocatable ocean models have been used together with the oil spill model, MEDSLIK-II, to provide ocean currents forecasts, possible oil spill scenarios, and drifters trajectories simulations. The models results together with the evaluation of their performances are presented in this paper. In particular, we focused this work on the implementation of the Interactive RElocatable Nested Ocean Model (IRENOM), based on the Harvard Ocean Prediction System (HOPS), for the Costa

Concordia emergency and on its validation using drifters released in the area of the accident. It is shown that thanks to the capability of improving easily and quickly its configuration, the IRENOM results are of greater accuracy than the results achieved using regional or subregional model products. The model topography, the initialization procedures, and the horizontal resolution are the key model settings to be configured. Furthermore, the IRENOM currents and the MEDSLIK-II simulated trajectories showed to be sensitive to the spatial resolution of the meteorological fields used, providing higher prediction skills with higher resolution wind forcing.

Responsible Editor: Tal Ezer

This article is part of the Topical Collection on the *5th International Workshop on Modelling the Ocean (IWMO) in Bergen, Norway 17-20 June 2013*

M. De Dominicis (✉)
Istituto Nazionale di Geofisica e Vulcanologia, Bologna, Italy
e-mail: michela.dedominicis@bo.ingv.it

S. Falchetti · F. Trotta · N. Pinardi · L. Giacomelli
Department of Physics and Astronomy, University of Bologna,
Bologna, Italy

E. Napolitano
ENEA, Rome, Italy

L. Fazioli · R. Sorgente
CNR-IAMC, Oristano, Italy

P. J. Haley Jr. · P. F. J. Lermusiaux
Massachusetts Institute of Technology, Cambridge, MA, USA

F. Martins
Universidade do Algarve, Faro, Portugal

M. Cocco
Tuscan Archipelago National Park, Portoferraio-Isle of Elba, Elba,
Italy

Keywords Relocatable model · Trajectory model · Drifters

1 Introduction

Relocatable models have been employed for emergency weather predictions, with results very useful for our society in the cases of severe weather outbreaks, hails, tornados, and hurricanes (e.g., Schroeder et al. 2006; Bender et al. 2007). In the ocean, tidal and shallow water models were likely the first relocatable models (e.g., Dietrich et al. 1993; Blain et al. 2002; Posey et al. 2008), again with multiple societal uses. A pioneering relocatable primitive-equation ocean model was that of the Harvard Ocean Prediction System (HOPS). It has been utilized for real-time shipboard predictions of ocean mesoscale circulations for the first time in the Iceland-Faeroe front region (Robinson et al. 1996). Subsequently, the HOPS relocatable model and its improved versions have been employed to issue real-time forecasts and analyze ocean dynamics in diverse regions of the world's oceans, including the Atlantic Ionian Stream and Strait of Sicily region (Robinson et al. 1999; Lermusiaux 1999), the

Strait of Gibraltar (Robinson and Sellschopp 2002), the Tunisia-Sardinia-Sicily region (Onken et al. 2002), and the Eastern Ligurian Sea (Robinson et al. 2003). Starting in the early 2000s, Maritime Rapid Environmental Assessment (MREA; Robinson and Sellschopp 2002) became one of the drivers for relocatable ocean modeling and forecasting. Such applications required the evaluation of the usefulness of predictions, especially the assessment of the predictive capability (Robinson et al. 2002) of the modeling systems. With this basis, more rigorous evaluations were completed in 2003 and 2004, for the relocatable Mini-HOPS modeling system applied to the Elba region and off the coast of Portugal (Leslie et al. 2008). A relocatable modeling approach for MREA04 has been also applied off the coast of Portugal (Ko et al. 2008). The relocatable HOPS system has been also integrated with the ocean general circulation model of the Mediterranean Forecasting System (MFS) (Russo and Coluccelli 2006). A review of the MREA concepts and applications is provided in Ferreira-Coelho and Rixen (2008). Relocatable models have been also employed recently for studying Lagrangian dynamics and dispersion in the Gulf of Mexico region (Wei et al. 2013a), which is an application related to our research.

Oil slicks caused by oil tanker/ships accidents compose a major source of hydrocarbon pollution for the marine and coastal environment (including seagrass beds, mangroves, algal flats, and coral reefs) and can jeopardize the functional integrity of the marine ecosystem (seabirds populations, fish communities, and marine mammals), as reported in Jackson et al. (1989), Piatt and Anderson (1996), Peterson et al. (2003). Since oil spill evolution depends on the winds, waves, sea temperature, and current conditions, oil spill management strategies need to be developed together with the improvement of meteorological, ocean, and wave forecasting models.

Pioneering examples of oil spill response systems were available during the *Braer* oil spill (Shetland Islands, UK, 1993) (Proctor et al. 1994) and the *Erika* oil spill (Brittany coast in the Bay of Biscay, France, 1999) (Daniel et al. 2001), which for the first time allowed operators to develop a response strategy rather than react only to observed information. Further examples of operational forecasting system for developing proper response strategies to oil spill emergencies were available during the *Prestige* oil spill crisis (Galicia coast, Spain, 2002) (Carracedo et al. 2006; Castanedo et al. 2006; Lermusiaux et al. 2007). In the Mediterranean Sea, an oil-spill decision-support system was developed during the largest oil-release accident in the Eastern Mediterranean, the Lebanese oil-pollution crisis, which occurred in mid-July 2006 (Coppini et al. 2011). During the recent largest accidental marine oil spill in the history of the petroleum industry, effective oil spill monitoring and modeling systems were critical to the rapid responses

achieved for the Deepwater Horizon event (Gulf of Mexico, 2010). The value of regional models (with improved resolution and topography) was demonstrated (Mariano et al. 2011), and an ensemble forecast system was developed with a focus on regional and global scales (Liu et al. 2011a, b). An example of a quasi-operational forecasting system composed by a finite-element model and a particle-tracking model was also implemented to provide high-resolution current velocity field and surface trajectories of the oil on the continental shelf and nearshore (Dietrich et al. 2012). However, the majority of the above oil spill rapid response systems have been based on regional or even basin-scale models. Thus, there is a need to analyze the possibility to use relocatable models that can be rapidly implemented in any region of the world, and to assess if they can provide accurate forecasts in a very short time, as required by the management of emergencies produced by oil spills or contaminants releases at sea.

An oil spill model is an important component in any emergency response or contingency plan. Oil spill numerical modeling started in the early 80s and, according to state-of-the-art reviews (ASCE 1996; Reed et al. 1999), a large number of numerical Lagrangian surface oil spill models have grown in the last 30 years. These models can vary from simple point source particle-tracking models, such as TESEO-PICHI (Castanedo et al. 2006; Sotillo et al. 2008), to complex models that attempt to comprehensively simulate the three-dimensional advection-diffusion-transformations processes that oil undergoes (Wang et al. 2008; Wang and Shen 2010). Some of the most sophisticated Lagrangian operational models are COZOIL (Reed et al. 1989), SINTEF OSCAR 2000 (Reed et al. 1995), OILMAP (Spaulding et al. 1994; ASA 1997), GULFSPILL (Al-Rabeh et al. 2000), ADIOS (Lehr et al. 2002), MOTHY (Daniel et al. 2003), MOHID (Carracedo et al. 2006), the POSEIDON OSM (Pollani et al. 2001 Nittis et al. 2006), OD3D (Hackett et al. 2006), the Seatrack Web SMHI model (Ambjörn 2007), MEDSLIK (Lardner et al. 1998, 2006), GNOME (Zelenke et al. 2012), OILTRANS (Berry et al. 2012), and MEDSLIK-II (De Dominicis et al. 2013a). Which type of model to use depends on the model availability in the area of interest and final objectives: from short-term forecasting to long-term impact assessment. The oil spill model used in this work is MEDSLIK-II (De Dominicis et al. 2013a) that is able to simulate the transport of surface drifters or the transport, diffusion, and transformations of a surface oil slick. It has been used extensively in the past to simulate oil spill accidents (Coppini et al. 2011) and/or drifter trajectories (De Dominicis et al. 2013b), and it proved to be reliable in short-term forecasting.

On January 13th, 2012, the *Costa Concordia* cruise ship hit a rocky outcrop and ran aground rolling onto its side as

it sailed near the Giglio island. With 2,500 t of fuel in its tanks, the Costa Concordia was immediately considered a high-risk accident for possible spills to occur. Though hypothetical, an oil spill scenario could not be totally discarded. MEDSLIK-II has been connected to operational regional (MFS; Pinardi and Coppini 2010) and subregional models, the Western Mediterranean (WMED; Olita et al. 2013) and the Tyrrhenian Sea (TYRR; Vetrano et al. 2010), to simulate scenarios of fuel leaks. In Fig. 1, the geographical domains of the models are presented. The oil spill scenarios and current forecasts have been provided every day and in real time to the Italian Coast Guard. In case of an oil spill, this information would have helped to plan the booms deployment, to place skimmers, to protect a particular piece of coast, or to intervene with airplanes or vessels. Moreover, a high-resolution, relocatable model, called Interactive RElocatable Nested Ocean Model (IRENOM) has been nested in MFS and its currents used as input to the MEDSLIK-II model. The hydrodynamics model core of IRENOM is based on the Harvard Ocean Prediction System (HOPS) (Robinson 1999), and the area of interest of this work is the north-western Mediterranean Sea where the Costa Concordia accident occurred (see Fig. 2).

To assess the accuracy of the oil spill simulations and of the ocean current predictions, a validation experiment with the release of four I-SPHERE drifters has been performed in the area of the accident. MEDSLIK-II has been used to simulate the drifter trajectories using the current fields output from different operational oceanographic models and from IRENOM. The latter has been shown to produce realistic drifter trajectories with higher accuracy than the coarser resolution regional and subregional models. In this work, the improvements in having high-resolution and

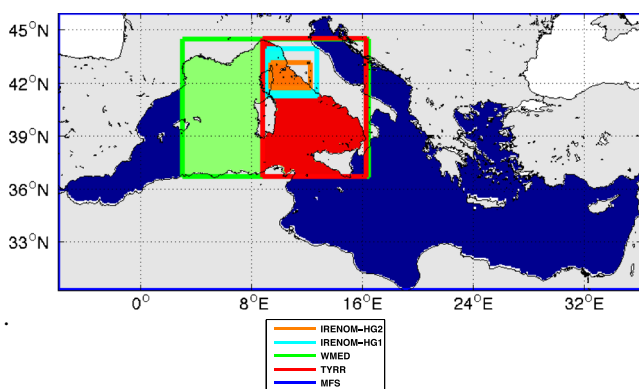


Fig. 1 OGCMs domains: the *blue box* is the MFS domain with 6.5-km resolution, the *green box* is the WMED domain with 3.5-km resolution, the *red box* is the TYRR domain with 2-km resolution, the *light blue box* is the IRENOM-HG1 domain with 3-km resolution, and the *orange box* is the IRENOM-HG2 domain with 2-km resolution (the zoom of the IRENOM domains is in Fig. 2). Coastline data from GSHHG (Global Self-consistent, Hierarchical, High-resolution Geography Database)

accurate forecasts of the ocean currents will be assessed and the sensitivity of the drifter trajectory forecasts to model configuration parameters and to wind fields with different resolutions will be analyzed.

The manuscript is organized as follows: Section 2 overviews the hydrodynamic models and oil spill model, together with the drifters data used for the validation; Section 3 shows the results of the operational support provided during the emergency; Section 4 presents the results of the IRENOM implementation and drifters validation experiments; and Section 5 offers the conclusions.

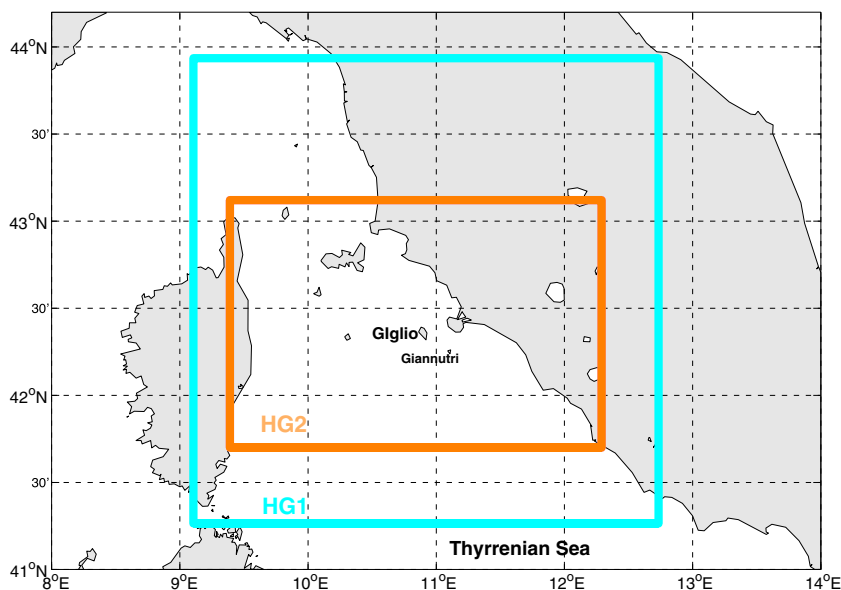
2 Models and data

2.1 IRENOM—interactive relocatable nested ocean model

The relocatable IRENOM ocean model is based on the hydrodynamics core model of HOPS (Robinson 1999), an integrated system of software for multidisciplinary oceanographic research developed by the physical oceanography group of Harvard University. As mentioned earlier, HOPS has been used in varied ocean regions for real-time ocean forecasting, data assimilation, and dynamics studies, especially in the Mediterranean Sea (Robinson et al. 1999, 2003; Lermusiaux 1999; Robinson and Sellschopp 2002; Onken et al. 2002). The initial version of the primitive-equation (PE) model of HOPS was a rigid-lid code, initialized based on procedures described in Lozano et al. (1996) and Robinson et al. (1996). Since that time, a free-surface version of HOPS was developed, numerical schemes were updated, and new algorithms were developed. This led to a new conservative finite-volume structured ocean model code with implicit two-way nesting for multiscale hydrostatic PE dynamics with a nonlinear free-surface (Haley and Lermusiaux 2010). With this multidisciplinary simulation, estimation and assimilation system, some of the modeling capabilities include balanced and nesting initialization and downscaling (Haley et al. 2013), multiresolution data-assimilative tidal prediction and inversion (Logotov and Lermusiaux 2008), fast-marching coastal objective analysis (Agarwal and Lermusiaux 2011), stochastic subgrid-scale models (e.g., Lermusiaux 2006), and data assimilation and adaptive sampling (Lermusiaux 2007).

In this manuscript, the core of the HOPS code employed is a free-surface, primitive-equation model and the prognostic variables are sea level, temperature, salinity, and total velocity discretized on an Arakawa B grid. The vertical coordinate adopted is a topography-following system, in particular a double-sigma system, chosen for accurate modeling of steep topography and the surface mixed layer. In the present set-up of HOPS, we use lateral open boundary conditions given in terms of an Orlanski (1976)

Fig. 2 IRENOM domains: the *light blue box* is the IRENOM domain with 3-km resolution identified by the label HG1 and the *orange box* is the IRENOM domain with 2-km resolution identified by the label HG2. Coastline data from GSHHG (Global Self-consistent, Hierarchical, High-resolution Geography Database)



radiation condition, applied to temperature, salinity, and velocity components. For sea level, a zero gradient boundary condition is chosen. The precipitation values are taken from climatologically monthly dataset CPC Merged Analysis of Precipitation (CMAP) (Xie and Arkin 1997). The surface heat and momentum fluxes are calculated interactively by the model from meteorological fields (see Section 2.3) using bulk formulae.

In this work, initial and lateral boundary conditions for IRENOM are taken only from the operational Mediterranean Forecasting System (MFS) model (Oddo et al. 2009) described later in Section 2.3. The variable temperature, salinity, and the total velocity are extracted from MFS daily mean fields and bilinearly interpolated onto the horizontal HOPS grid and mapped from flat (z-levels) to terrain-following levels.

The IRENOM is configured through a user friendly Graphical User Interface (GUI). Figure 3 shows the flowchart of the IRENOM implementation through the GUI. After the acquisition of the necessary input forcings (MFS currents and ECMWF or SKIRON winds, see Section 2.3) for the selected period, the GUI software executes two simultaneous processes: the generation of the grid and the input data conversion into IRENOM format. The preparation of the grid is divided into various phases. First, the horizontal grid is defined on the basis of the coordinates and resolution indicated by the user. Then, through the GUI, the user can choose different positions of the vertical levels by varying some parameters, such as shallowest depth to retain (vertical clipping), number of levels or the slope. The vertical grid and the land-sea mask are generated automatically. The user may also manually change the default land-sea mask by using the GUI, i.e., introduce or remove islands in the domain, depending on the resolution to be

achieved or the physical processes to be resolved. Then, the interpolation of the father model currents on the IRENOM grid is performed to generate the initial condition and boundary conditions. At this point, the simulation can be performed. At the end of the simulation, the GUI allows the

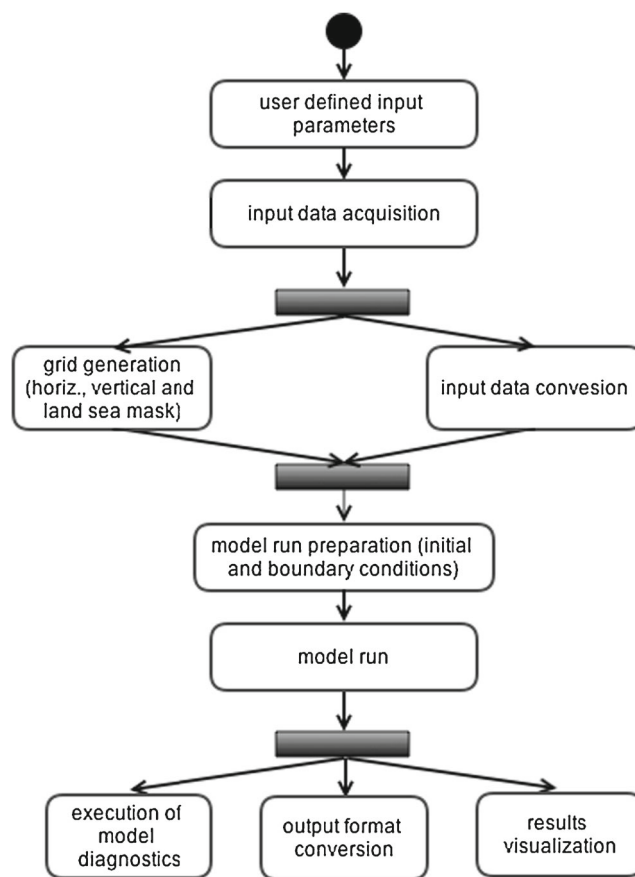


Fig. 3 Flowchart of the IRENOM implementation through the GUI

visualization of the results, the transformation of the output in different formats, and the model diagnostics.

Before describing the oil spill model (Section 2.2), we note that downscaling and nesting of different regional models has been successfully completed before (e.g., Onken et al. 2005; Ramp et al. 2011, and Lermusiaux et al. 2011). In Onken et al. (2005), a degradation of the interior solution has been reported for long runs. Furthermore, the use of data assimilation in operational oceanography can make it difficult to cleanly assess the effect of nesting procedures. In our case, even though we employ a one-way nesting scheme for the downscaling of the operational MFS, two-way nesting could have been used. For a review on nesting schemes, we refer to Debreu and Blayo (2008). Recent nesting schemes relevant to our application are obtained in Haley and Lermusiaux (2010) and Mason et al. (2010). In particular, the implicit two-way nesting of Haley and Lermusiaux (2010) could be combined with nesting initialization and downscaling schemes (Haley et al. 2013), which improve the consistency among model fields and reduce unphysical transients due to nesting of multiple model types.

2.2 The oil spill and trajectory model: MEDSLIK-II

The oil spill model code MEDSLIK-II (De Dominicis et al. 2013a, b) is now a freely available community model (<http://gnoo.bo.ingv.it/MEDSLIKII>). It is designed to be used to predict the transport and weathering (evaporation, dispersion, spreading, and beaching, as described in De Dominicis et al. 2013a) of an oil spill or to simulate the movement of a floating object. MEDSLIK-II is a Lagrangian model, which means that the oil slick is represented by a number N of constituent particles that move by advection due to the hydrodynamics currents and disperse by Lagrangian turbulent diffusion. At the surface, the horizontal current field used in the Lagrangian model is taken to be the sum of different components:

$$d\mathbf{x}_k(t) = [\mathbf{U}_C(x_k, y_k, t) + \mathbf{U}_W(x_k, y_k, t) + \mathbf{U}_S(x_k, y_k, t) + \mathbf{U}_D(x_k, y_k, t)] dt + d\mathbf{x}'_k(t) \tag{1}$$

where \mathbf{U}_C is the wind, buoyancy, and pressure-driven large-scale current velocity field, \mathbf{U}_W is the local wind velocity correction term, \mathbf{U}_S is the wave-induced current term (Stokes drift velocity), \mathbf{U}_D is the wind drag correction due to emergent part of the objects at the surface, and $d\mathbf{x}'_k(t)$ is the displacement due to the turbulent diffusion. The local wind correction term \mathbf{U}_W and the Stokes drift \mathbf{U}_S are written as follows:

$$\begin{aligned} U_W &= \alpha(W_x \cos \beta + W_y \sin \beta) \\ V_W &= \alpha(-W_x \sin \beta + W_y \cos \beta) \end{aligned} \tag{2}$$

$$\begin{aligned} U_S &= D_S \cos \vartheta \\ V_S &= D_S \sin \vartheta \end{aligned} \tag{3}$$

where (W_x, W_y) are the wind velocity components at 10 m, $\vartheta = \arctg\left(\frac{W_x}{W_y}\right)$ is the wind direction, and D_S is the Stokes drift velocity intensity in the direction of the wave propagation at the surface, defined as follows:

$$D_S(z = 0) = 2 \int_0^\infty \omega k(\omega) S(\omega) d\omega \tag{4}$$

where ω is angular frequency, k is wave-number, and $S(\omega)$ is wave spectrum. Using this parametrization, we assume that wind and waves are aligned and the waves are generated only by the local wind (swell process is not considered).

When \mathbf{U}_C is provided by oceanographic models that resolve the upper ocean layer dynamics (1–3-m resolution and turbulence closure submodels), the term \mathbf{U}_C contains a satisfactory representation of surface ageostrophic currents, and the \mathbf{U}_W term may be neglected (in this work \mathbf{U}_W has been always set equal to 0). The wind drag correction, \mathbf{U}_D , is associated with the leeway (windage) of a floating object, defined as the drift associated with the wind force on the overwater structure of the object. As defined by Röhrs et al. (2012) and Isobe et al. (2011), the leeway-drift velocities can be parametrized as follows:

$$\mathbf{U}_D = \sqrt{\frac{\rho_a A_a C_{da}}{\rho_w A_w C_{dw}}} \mathbf{W} = \gamma \mathbf{W} \tag{5}$$

where ρ , A , C_d are the fluid density, projected areas of the object, and drag coefficient, respectively, and subscripts a and w denote the air and seawater environments. The parameter γ cannot be calculated directly because the drag coefficients C_{da} and C_{dw} are Reynolds numbers dependent and are not straightforward to use at the air-sea interface with wave disturbances (Röhrs et al. 2012). Field experiments performed by Röhrs et al. (2012) suggest to use γ in the range 0.003–0.01. In the simulation experiments of single drifter trajectories (see Section 4), γ has been set equal to 0.01, thus \mathbf{U}_D is about 1 % of the wind velocity. While simulating a real oil slick (see Section 3), the leeway-drift velocity has been omitted, $\mathbf{U}_D = 0$.

The turbulent diffusion is parameterized with a random walk scheme as follows:

$$d\mathbf{x}'_k(t) = \sqrt{2\mathbf{K}dt} \mathbf{Z} \tag{6}$$

where \mathbf{K} is the turbulent diffusion diagonal tensor and \mathbf{Z} is a vector of independent random numbers used to model the Brownian random walk processes chosen for the parametrization of turbulent diffusion. The turbulent diffusion is considered to be horizontally isotropic and the three

diagonal components of \mathbf{K} are indicated by K_h , K_h , K_v . In the simulation experiments of a real oil slick (see Section 3), K_h has been set to $2 \text{ m}^2\text{s}^{-1}$, in the range $1\text{--}100 \text{ m}^2\text{s}^{-1}$ indicated by ASCE (1996) and De Dominicis et al. (2012), while K_v has been set to $0.01 \text{ m}^2\text{s}^{-1}$ in the mixed layer (assumed to be 30-m deep) and below it to $0.0001 \text{ m}^2\text{s}^{-1}$. When simulating single drifter trajectories (see Section 4), the diffusivity coefficients are set to zero.

When simulating a real oil slick, MEDSLIK-II allows the processes of spreading, evaporation, dispersion, emulsification, and coastal adsorption to evolve. When the oil first enters the sea, the slick spreads on the sea surface because of gravitational forces. As it is transported, lighter oil components disappear through evaporation and heavier ones emulsify with the water or are dispersed in the water column. MEDSLIK-II is also able to take into account adsorption of oil by the coast should the slick reach it. The full description of the model formulation can be found in De Dominicis et al. (2013a).

2.3 The larger scale current models and the atmospheric forcing

By way of inputs, both IRENOM and MEDSLIK-II require data on sea currents, sea surface temperature, and atmospheric forcing. For the ocean currents, MEDSLIK-II has been connected to regional (MFS; Pinardi and Coppini 2010) and subregional operational current models, such as the Western Mediterranean (WMED; Olita et al. 2013) and the Tyrrhenian Sea (TYRR; Vetrano et al. 2010). Furthermore, IRENOM has been nested in MFS and MEDSLIK-II used as input the IRENOM currents to examine the trajectory simulations skill of the relocatable model with respect to all the others. The main characteristics of the OGCMs presented in this Section are listed in Table 1 and geographical domains are shown in Fig. 1.

The MFS system (<http://gnoo.bo.ingv.it/mfs/myocean/>) is composed of an OGCM (Oddo et al. 2009) covering the entire Mediterranean Sea and an assimilation scheme (Dobricic and Pinardi 2008) which corrects the model's initial guess with all the available in situ and satellite observations. The model code is Nucleus for European

Modelling (NEMO), a detailed description of the code can be found in Madec (2008). NEMO is coupled with the wave model WWIII (WAVEWATCH III; Tolman 2009; Clementi et al. 2013). NEMO and WWIII have been implemented in the Mediterranean at $1/16^\circ$ (approximately 6.5 km) horizontal resolution and 71 unevenly spaced vertical levels. The model is forced by momentum, water, and heat fluxes interactively computed by bulk formulae using the 6-hourly, 0.25° horizontal-resolution operational analyses from the European Center for Medium-Range Weather Forecasts (ECMWF), and the model predicted surface temperatures (details of the air-sea physics are in Tonani et al. 2008). Operationally, MFS produces daily and hourly mean forecasts. Once a week, the system also provides daily mean and hourly analyses, which are best estimates of oceanographic conditions. The MFS basin scale output provides initial and lateral boundary conditions for higher-resolution subregional models in addition to MFS.

WMED (<http://www.seaforecast.cnr.it/en/fl/wmed.php>) is a three-dimensional primitive equation hydrodynamic model based on the Princeton Ocean Model (POM; Blumberg and Mellor 1987). POM solves the equations of continuity, motion, conservation of temperature, salinity, and assumes hydrostatic and Boussinesq approximation. WMED covers the western Mediterranean area (from 3.0°E to 16.47°E in longitude and from 36.7°N to 44.48°N in latitude) with a horizontal grid resolution of $1/32^\circ$ (approximately 3.5 km). It uses 30 vertical sigma levels, denser at the surface following a logarithmic distribution. The model is initialized with a cold start using dynamically balanced forecast fields from MFS, through a downscaling of the forecast fields produced by the basin-scale circulation models. In this case, the forecasts result to be closely dependent on the accuracy of the MFS fields and on the methodology used for interpolating the regional-scale model on the model numerical grid (horizontal and vertical). This method of initialization is also known as a *slave mode* forecasting mode. The main disadvantage of this methodology has to do with the different resolutions, both horizontal and vertical, of the regional and basin-scale models. Incorrect dynamic balancing of interpolated fields leads, in fact, to

Table 1 OGCMs characteristics and domains

Model name	Domain	Resolution	Numerical code	Father model
MFS	-6.0°E – 36.25°E ; 30.25°N – 46.0°N	$1/16^\circ$	NEMO	–
TYRR	8.81°E – 16.29°E ; 36.68°N – 44.5°N	$1/48^\circ$	POM	MFS
WMED	3.0°E – 16.47°E ; 36.7°N – 44.48°N	$1/32^\circ$	POM	MFS
IRENOM-HG1	9.11°E – 12.73°E ; 41.26°N – 43.93°N	$1/27^\circ$ (Lon) – $1/37^\circ$ (Lat)	HOPS	MFS
IRENOM-HG2	9.39°E – 12.29°E ; 41.70°N – 43.12°N	$1/41^\circ$ (Lon) – $1/56^\circ$ (Lat)	HOPS	MFS

the generation and propagation of gravity waves during the spin-up time (Auclair et al. 2000). To minimize this noise in the downscaling procedure, a best-interpolation method based on Variational Initialization and FORcing Platform (VIFOP) variational analysis is used (Gaberšek et al. 2007). MFS also provides boundary conditions through a simple off-line one-way asynchronous nesting as described in details in Sorgente et al. (2003). Surface fluxes are computed through bulk formulas (Castellari et al. 1998) from the 6-hourly atmospheric analyses from ECMWF at 0.25° of resolution. WMED provides a daily 5-day prediction of water currents, temperature, and salinity at different water depths as daily and hourly mean output.

TYRR (<http://utmea.enea.it/research/MEDMOD/>) is one of the MFS nested models covering the area of Tyrrhenian Sea (from 8.81°E to 16.29°E in longitude and from 36.68°N to 44.50°N in latitude) with a horizontal grid resolution of $1/48^\circ$ (approximately 2 km). The numerical model used is Princeton Ocean Model (POM) (Blumberg and Mellor 1987; Mellor 2004). The vertical grid consists of 40 sigma levels that are smoothly distributed along the water column, with appropriate thinning designed to better resolve the surface and intermediate layers. Initial conditions are taken from MFS analysis as follows: every week a hindcast run of 7 days is performed, it is forced by the ECMWF analysis fields and uses the MFS analysis fields for initial and boundary conditions. After this spin-up period of 7 days, for the following week, the TYRR system provides a daily 5-day prediction of water currents, temperature, and salinity at different water depths as daily and hourly mean output, starting from the restart of the forecast of the previous day. Boundary conditions are obtained by interpolating on the TYRR grid the temperature, salinity, velocities, and surface elevation fields produced by MFS.

For the atmospheric forcing, a sensitivity analysis of the IRENOM currents and the MEDSLIK-II trajectory simulation skills to the meteorological fields resolution has been performed. The first atmospheric forcing used comes from the ECMWF model output (0.25° and 6 h), which is the forcing used operationally by the regional, MFS, and subregional models, WMED and TYRR. The second one is the higher-resolution atmospheric model SKIRON, with 0.025° horizontal resolution and for this work with temporal resolution of 6 h. SKIRON (Spyrou et al. 2010) is a modeling system developed at the University of Athens from the AM&WFG (Kallos et al. 1997, 2006). The atmospheric model is based on the ETA/National Centers for Environmental Prediction (NCEP) model, which was originally developed by Mesinger (1984) and Janjic (1984) at the University of Belgrade. Details on the various model parameterization schemes can be found in the abovementioned studies and references therein.

2.4 Drifters data

The drifters are oceanographic instruments used to study the surface circulation and oceanographic dynamics; they are designed to be transported by ocean currents, and these characteristics make them useful tools for the validation of hydrodynamic models (Barron et al. 2007; Huntley et al. 2011; Liu and Weisberg 2011) and oil spill/trajectory models (Reed et al. 1994; Al-Rabeh et al. 2000; Price et al. 2006; Caballero et al. 2008; Sotillo et al. 2008; Cucco et al. 2012; Liu et al. 2011c; Mariano et al. 2011). Oil spill-following surface drifters (i-SPHERE) (Price et al. 2006) are 39.5 cm diameter spheres designed on the basis of earlier experiments carried out in the late 1980s and early 1990s.

During the Costa Concordia emergency, drifters were deployed south-eastward of the Giglio island (Fig. 4). The four drifters were released on the 14th of February 2012 and recovered 24 h later. As shown in Fig. 4, the buoys had a linear arrangement from northeast to southwest and an average distance of about 7 km between Giglio and Giannutri Island. These data were used to evaluate the accuracy of the ocean currents provided by MFS, WMED, and TYRR. Then, the drifters were used to validate the different IRENOM model

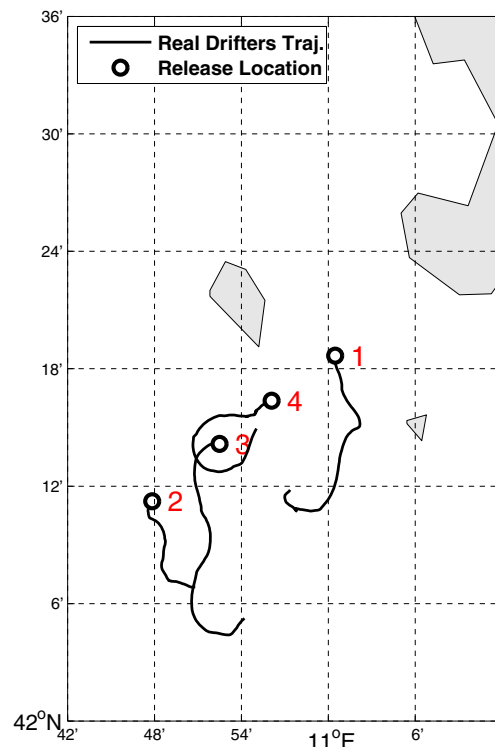


Fig. 4 Real drifters trajectories (black lines) from 14th February at 9:00 UTC to 15th February at 9:00 UTC

settings, in order to understand the improvements in simulating the ocean state derived from a nested relocatable model approach.

2.5 Lagrangian trajectory evaluation metrics

Two metrics will be used to quantitatively evaluate the accuracy of the Lagrangian trajectory simulations. The first metric is the Lagrangian separation distance $d_i(\mathbf{x}_s(t_i), \mathbf{x}_o(t_i))$ between the observed and the simulated trajectories, where d_i is the distance at the selected time t_i , after a reference time t_0 , between the simulated drifter position, \mathbf{x}_s , and the observed positions, \mathbf{x}_o . The second metric is the Liu and Weisberg (2011) skill score. It is defined as an average of the separation distances weighted by the lengths of the observed trajectories as follows:

$$s(t_i) = \frac{\sum_{t=t_0}^{t_i} d_i(\mathbf{x}_s(t), \mathbf{x}_o(t))}{\sum_{t=t_0}^{t_i} l_{oi}(\mathbf{x}_o(t_0), \mathbf{x}_o(t))} \quad (7)$$

where l_{oi} is the length of the observed trajectory at the corresponding time, t_i , after a reference time t_0 . Such weighted average tends to reduce the evaluation errors that may rise using only the purely Lagrangian separation distance. The s index can be used to define a model skill score as follows:

$$ss(t_i) = \begin{cases} 1 - \frac{s(t_i)}{n} & (s \leq n) \\ 0 & (s > n) \end{cases} \quad (8)$$

where n is a tolerance threshold. In this work, as suggested by Liu and Weisberg (2011), we used $n = 1$, this corresponds to a criterion that cumulative separation distance should not be larger than the associated cumulative length of the drifter trajectory. The higher the ss value, the better the performance, with $ss = 1$ implying a perfect fit between observation and simulation and $ss = 0$ indicating that the model simulations have no skill.

3 The operational support during the emergency: the multimodel approach

On January 13, 2012, only hours after leaving the Italian port of Civitavecchia, the Costa Concordia cruise ship with more than 4,200 passengers and crew on board hit a rocky outcrop, ran aground, and rolled onto its side as it sailed off the Giglio Island. Italian Authorities (Coast Guards and Civil Protection) immediately reacted by deploying search and rescue and risks mitigation measures, including environmental risks. With about 2,500 t of fuel in its tanks, the concern about the potential environmental impact was high. In case of failure of the debunkering operation, a spillage might have polluted the Tuscan Archipelago National Park, a marine environmental protected area. Every day, starting

from the 16th of January and until the fuel unloading operations finished, the coupled hydrodynamics and MEDSLIK-II system was run to produce scenarios of the possible oil spill from the Costa Concordia. MEDSLIK-II used the currents (hourly fields) provided every day by the operational ocean models available in the area: MFS, TYRR, and WMED. Thanks to these data, a fuel leak can be simulated to forecast the possible fuel dispersion into the sea and along the coast. The position of the possible oil spill coincides with the ship position in the proximity of the Giglio Island harbor. The amount of oil spilled was decreased on the basis of the quantity debunkered. Daily bulletins were provided to the Italian Coast Guard Operational Center. Those bulletins presented the forecasts of the currents, wind and oil dispersion at surface up to 72 h after the possible spill, supposed to be released continuously in 72 h. Though hypothetical, an oil spill scenario could not be totally discarded, and this information would have been crucial for helping local maritime authorities to be better prepared in setting up prevention measures and optimizing cleaning operations. The bulletin dissemination to other competent authorities was managed under the responsibility of the Italian Coast Guard, and it complemented the information coming from European services (e.g., oil spill detection and monitoring from EMSA, the European Maritime Safety Agency).

Figure 5 shows an example of the information contained into the bulletin provided to the competent authorities. When all the models are in agreement, we might be more confident in the accuracy of the forecasts. Nevertheless, there were times in which the three models gave very different predictions, as shown in Fig. 5. Reasons for the different model forecasts may be due to different numerical code (NEMO, POM), specific grids, parameterizations, data assimilation schemes, and domains. Commonalities are that both WMED and TYRR are nested into MFS, but using different initialization procedure (see Section 2.3). WMED with a daily initialization from MFS cannot deviate much from MFS, while TYRR model uses an initialization period of 7 days, allowing the model to produce its own dynamics. During the Costa Concordia emergency, only a qualitative comparison of the model results has been performed and the different forecasts have been not produced from true ensemble prediction systems based on dynamics. Despite this, a similar methodology was implemented during the Deepwater Horizon oil spill (Liu et al. 2011b, c), and it demonstrated to provide some degree of confidence that any single model alone might not. Although super-ensemble techniques for ocean (Rixen et al. 2009) and weather forecasting (Krishnamurti et al. 2000a, b) are widely used, few examples on using ocean ensembles in Lagrangian trajectory models are available. It has been demonstrated that the trajectories ensemble can generate important uncertainty information in addition to predicting the drifter trajectory

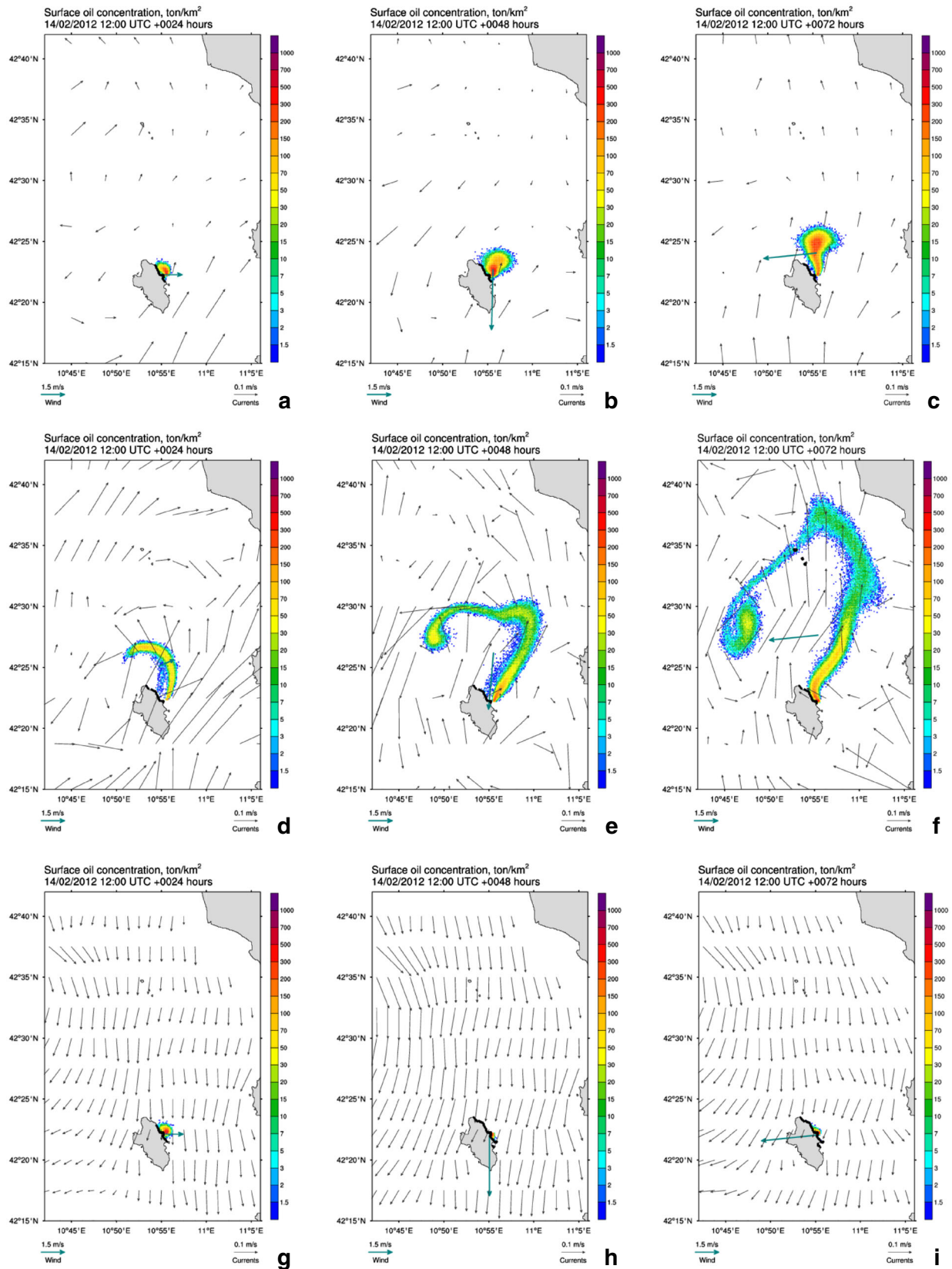


Fig. 5 The 14th of February 2012 bulletin example: the surface oil concentration 24, 48, and 72 h after the possible spill using MFS (a–c), WME (d–f), and TYRR (g–i). Oil concentration is visualized with

colors from blue to purple in t/km^2 . Oil on the coast is highlighted in black. Currents (black arrows) and wind (green arrow) forecasts are shown in the background

with higher accuracy, in contrast to a single ocean model forecast (Wei et al. 2013b). How to combine models results is not obvious and some recent works have been done on this issue. One methodology is the hyper-ensemble technique (Rixen and Ferreira-Coelho 2007; Rixen et al. 2008; Vandenbulcke et al. 2009), which combines multiple model of different physical processes (ocean currents, winds, and waves) and then performs the trajectory simulations using the combined product. The optimal combination is obtained during a training period by minimizing the distance between modeled and observed trajectories and requires comprehensive observational networks. Another option is to combine a posteriori the modeled trajectory obtained using the different velocity fields (Scott et al. 2012). In the future and with a larger drifters dataset, these methodologies will be explored.

Giving the errors inherent to any model, its forcing fields and its initialization, a validation exercise has been organized to assess the quality of produced forecasts, as described in Section 2.4. As shown in Table 2, nine simulations have been done to evaluate the models performances and the sensitivity of the oil spill model to some parameterizations and to the forcing fields. We performed a first set of simulations using only the hourly surface currents, U_C term of Eq. 1, from MFS, TYRR, and WMED. Then, we carried out a second set of experiments to take into account the Stokes drift effect, U_S term of Eq. 1. The last set of simulations has been performed adding also the wind drag correction, U_D term of Eq. 1, which is equal to 1 % of the wind velocity intensity. In Fig. 6, the comparison between one of the real drifters trajectories (buoy 1 of Fig. 4) and the simulated trajectories is shown. Qualitatively, we can see that the simulated trajectories using MFS and WMED go in the wrong direction. Using TYRR currents, the simulated trajectory are in better agreement with the observed one, but without adding the wind drag correction and the Stokes drift correction (Fig. 6a, b), the displacement of the simulated drifter is underestimated. The best results are obtained with the experiment TYRR-CSD (Fig. 6c) that shows a higher

displacement of the simulated drifter in the correct direction. The separation distance, d_{24h} , and the skill score, ss_{24h} , after 24 h of simulation have been calculated for all buoys. In Table 3, the values obtained for buoy 1 are listed, together with the average over the four buoys. Exp. TYRR-CSD shows the lowest separation distance (4.15 km) and highest skill score (0.59) in reproducing buoy 1 trajectory, confirming that the best results are obtained using the TYRR currents and using the Stokes drift and wind drag terms. In Fig. 7, the decomposition of the total velocity that drives the simulated buoy 1 in the Exp. TYRR-CSD is shown. It is found that the effect of the wave correction, U_S , and wind drag correction, U_D , can be, as in this case, of the same order of magnitude of the current velocity, U_C .

4 Validation of the relocatable model using drifters trajectories

During the Costa Concordia emergency, the IRENOM relocatable model has been used in order to provide high/very high-time and space resolution forecasts starting from operational large-scale circulation models. The sensitivity of the relocatable model implementation to some model settings, summarized in Table 4, is analyzed, and the results are validated using the surface drifters.

In order to test the sensitivity to different horizontal grid resolutions, two horizontal domains are chosen. The first domain covers the region from 41.26°N to 43.93°N and from 9.11°E to 12.73°E. The horizontal grid resolution is approximately 3 km and consists of 100 × 100 points. The second domain covers the region from 41.70°N to 43.12°N and from 9.39°E to 12.29°E. The horizontal grid resolution is approximately 2 km and consists of 120 × 80 points. The two domains are referred in Tables 1 and 4 as HG1 and HG2, respectively, and are shown in Fig. 2. Both configurations have 25 double sigma levels. The bathymetry for both configurations has been obtained from the US Navy

Table 2 Sensitivity experiments of modeled trajectories to different OGCMs currents fields and to the particle trajectory equation terms

Exp. name	Current field	U_C	U_S	U_W	U_D
MFS-C	Hourly Surface Currents MFS	Yes	No	No	No
WMED-C	Hourly Surface Currents WMED	Yes	No	No	No
TYRR-C	Hourly Surface Currents TYRR	Yes	No	No	No
MFS-CS	Hourly Surface Currents MFS	Yes	Yes	No	No
WMED-CS	Hourly Surface Currents WMED	Yes	Yes	No	No
TYRR-CS	Hourly Surface Currents TYRR	Yes	Yes	No	No
MFS-CSD	Hourly Surface Currents MFS	Yes	Yes	No	Yes
WMED-CSD	Hourly Surface Currents WMED	Yes	Yes	No	Yes
TYRR-CSD	Hourly Surface Currents TYRR	Yes	Yes	No	Yes

Table 3 Results of Table 2 experiments in terms of separation distances and skill scores

Exp. name	Buoy1 d_{24h}	Buoy1 ss_{24h}	Mean d_{24h}	Mean ss_{24h}
MFS-C	16.73 km	0	14.93 km	0.09
WMED-C	23.06 km	0	20.56 km	0
TYRR-C	9.34 km	0.35	13.16 km	0.33
MFS-CS	13.68 km	0.15	11.78 km	0.30
WMED-CS	20.15 km	0	15.93 km	0.13
TYRR-CS	6.10 km	0.50	11.51 km	0.48
MFS-CSD	11.05 km	0.28	9.55 km	0.46
WMED-CSD	17.63 km	0.06	13.01 km	0.35
TYRR-CSD	4.15 km	0.59	10.34 km	0.54

unclassified 1 min bathymetric database DBDB-1, by linear interpolation of the depth data into the model grid.

One of the main differences between the IRENOM configurations and MFS is the topography. Due to the low resolution of the MFS model, the Giglio and Giannutri Islands (see Fig. 2) is not reproduced in the MFS topography, while in the IRENOM model, the land/sea mask has been correctly implemented. Thus, it is necessary to initialize the IRENOM model some days before the day of the deployment of the drifters to let the model correctly reproduce the dynamic of the current between the islands, which drives the drifters transport. The sensitivity to the initialization time (spin-up time) is extensively examined in this work. The spin-up time is defined as the time needed by an ocean model to reach a state of physical equilibrium under the applied forcing. The results cannot be trusted until this equilibrium is reached due to spurious noise in the

numerical solution. The sensitivity to a model initialization of 3, 5, and 7 days is tested as indicated in Table 4, where these spin-up times are labeled T11, T09, and T07, respectively.

Next, in order to test the influence of the topography on the model results, a simulation with alternating direction Shapiro filters is done, see label YS in Table 4. In this case, a fourth-order Shapiro filter is applied and the number of filter applications is set to 2. The model sensitivity to the shallowest allowed topography is also tested by using a topography clipping value of 5 m (see label C5 in Table 4) against the standard 10-m value used for all the other model runs.

The above runs have been performed using the ECMWF model output with 0.25° resolution, which is the forcing used operationally by MFS, WMED, and TYRR. Such coarse atmospheric model gives forcing only every approximately 12×12 grid points of the IRENOM model with

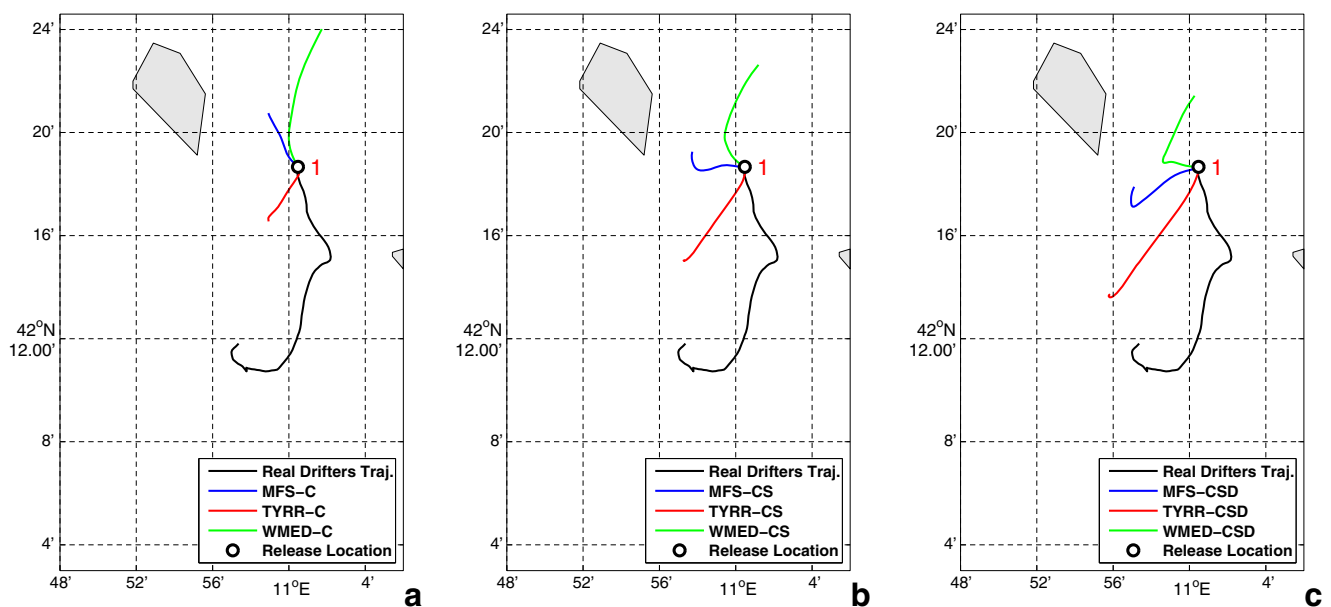
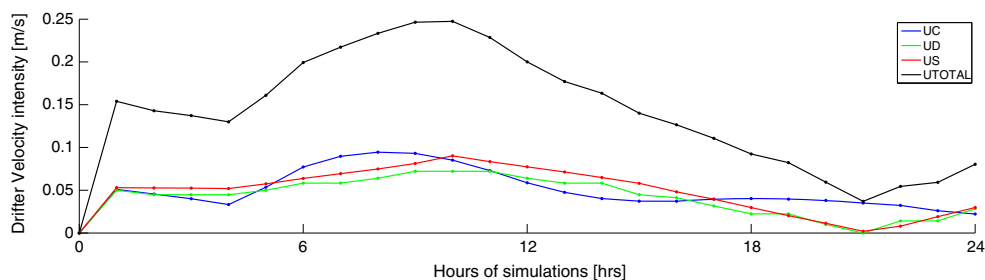


Fig. 6 Drifter 1 observed trajectory (black line) and the MEDSLIK-II trajectories using MFS (blues lines), WMED (green lines), and TYRR (red lines). **a** Using only the surface current term, **b** using the surface

current term and the Stokes drift correction, **c** using the surface current term, the Stokes drift, and the wind drag

Fig. 7 Decomposition in its three components (currents, Stokes drift, and wind drag) of the total velocity intensity used in Exp. TYRR-CSD



2-km resolution, and it might not give a realistic representation of the wind field forcing for a high-resolution hydrodynamic model. Thus, a sensitivity analysis of the 2-km configuration of the IRENOM model to the horizontal resolution wind forcing has been performed by running IRENOM forced by the SKIRON winds with a resolution of 0.025° . The experiments are indicated in the Table 4 with the label SKI. In theory, higher-resolution wind forcing should give better predictions, but it is not obvious because if the higher resolution forcing does not represent well the smaller weather scales, island structure, etc., the fine-grid ocean simulation with higher resolution forcing may be worse than with the coarse forcing.

Finally, the four buoys have been simulated using the MEDSLIK-II model forced by the currents coming from the 11 different IRENOM configurations. The trajectory simulations have been performed using the currents, the Stokes drift, and the wind drag, because, as it was found in Section 3, U_S and U_D should not be neglected. To be consistent with the IRENOM current fields, U_S and U_D are calculated by MEDSLIK-II using the same wind forcing used to force the IRENOM model.

Figure 8a–c shows the IRENOM sea surface current fields obtained with a horizontal resolution of 3 km, ECWMF 0.25° wind forcing, and with a spin-up time of 7 days (a), 5 days (b), and 3 days (c). A greater spin-up

time causes the development of stronger currents especially south of Elba Island and finer spatial scales have a greater time to develop, as is the case of the circulation pattern north of Elba Island. To decide which spin-up time should be used, the general practice (Simoncelli et al. 2011) would suggest to choose the spin-up time which allows the ocean model to reach a state of physical equilibrium, i.e., Total Kinetic Energy (TKE) plateau reached. Figure 9 shows the ratio between the (TKE), on the target day 14 February at 12:00 UTC, of the relocatable model and that of the father model MFS as a function of the spin-up time. The IRENOM model with 3-km resolution does not reach a plateau, as shown in Fig. 9 (blue line), but the slope of the curve diminished between 5 and 6 days of spin-up time. This behavior would suggest better trajectory predictions using the current fields of IRENOM obtained with an initialization time of at least 5 days. However, the circulation pattern depicted in Fig. 8a–c shows that a spin-up time longer than 3 days breaks the flow continuity that is observed along the channel, leading to worse trajectories predictions (presented later in this Section).

Figure 8d shows the sea surface current fields with a horizontal resolution of 2 km with a spin-up time of 3 days (5 and 7 days spin-up time results are not shown) and forced by ECWMF 0.25° wind forcing. With this finer horizontal grid resolution, different spatial scales develop in

Table 4 IRENOM sensitivity experiments to different model settings

Exp. name	Horiz. Resol.	Spin-up	Vertic. Clipp.	Shapiro	Wind forcing
HG1-T11	3 km	3 days	10 m	No	ECMWF 0.25°
HG1-T09	3 km	5 days	10 m	No	ECMWF 0.25°
HG1-T07	3 km	7 days	10 m	No	ECMWF 0.25°
HG2-T11	2 km	3 days	10 m	No	ECMWF 0.25°
HG2-T09	2 km	5 days	10 m	No	ECMWF 0.25°
HG2-T07	2 km	7 days	10 m	No	ECMWF 0.25°
HG2-T11-YS	2 km	3 days	10 m	Yes	SKIRON 0.025°
HG2-T11-C5	2 km	3 days	5 m	No	SKIRON 0.025°
HG2-T11-SKI	2 km	3 days	10 m	No	SKIRON 0.025°
HG2-T09-SKI	2 km	5 days	10 m	No	SKIRON 0.025°
HG2-T07-SKI	2 km	7 days	10 m	No	SKIRON 0.025°

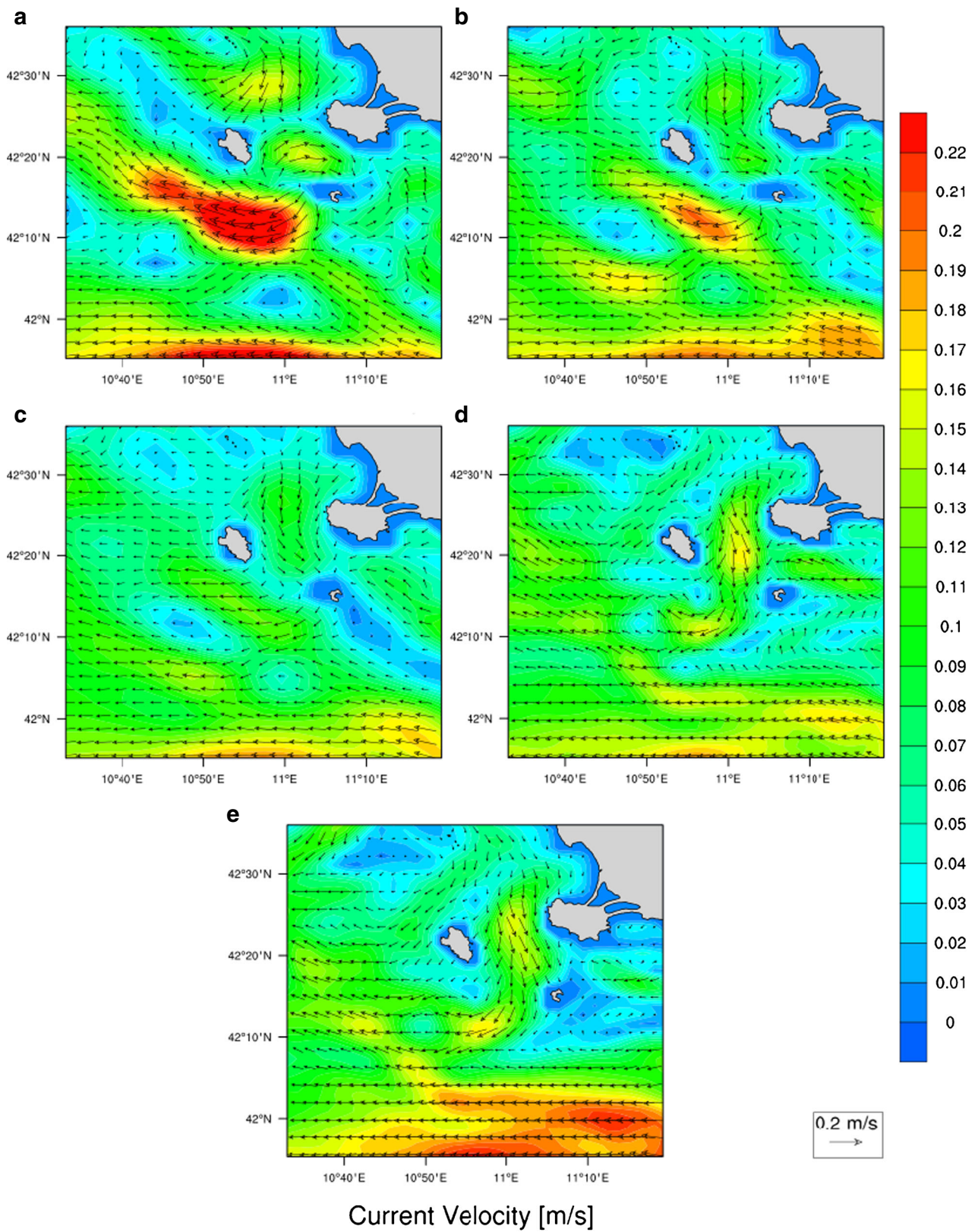


Fig. 8 Sensitivity of the IRENOM current fields to the spin-up time, model numerical horizontal grid resolution, and wind forcing horizontal resolution. Currents field at the 14 February 2012 12:00 UTC: 7-days spin-up, 3 km, and ECMWF 0.25° (a); 5-days spin-up, 3 km,

and ECMWF 0.25° (b); 3-days spin-up, 3 km, and ECMWF 0.25° (c); 3-days spin-up, 2 km, and ECMWF 0.25° (d); and 3-days spin-up, 2 km, and SKIRON 0.025° (e)

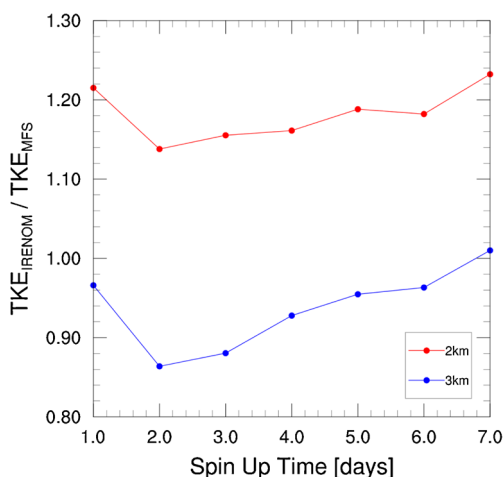


Fig. 9 Mean kinetic energy ratio between IRENOM relocatable model and MFS father model calculated on target day 14 February 12:00 UTC as function of spin-up time

comparison to the coarser 3-km resolution. In particular, considering that at the time of drifters release a wind of about 5 m/s was blowing from north east, the development of weaker currents in the calm lee behind the Elba Island is expected. This is actually the case for the finer grid resolution, in contrast to the current field observed in Fig. 8a–c. The ratio between the TKE, on the target day 14 February at 12:00 UTC, of the relocatable model with 2-km resolution and that of the father model MFS as a function of the spin-up time is shown in Fig. 9 (red line); with this resolution, the slope of the curve is lower than in the IRENOM configuration with 3-km resolution, suggesting that the plateau is almost reached after 3 days.

The sensitivity of the IRENOM configuration with 2-km resolution to the atmospheric model horizontal resolution has been also investigated, and in Fig. 8e, the sea surface current fields, obtained with a spin-up time of 3 days, is

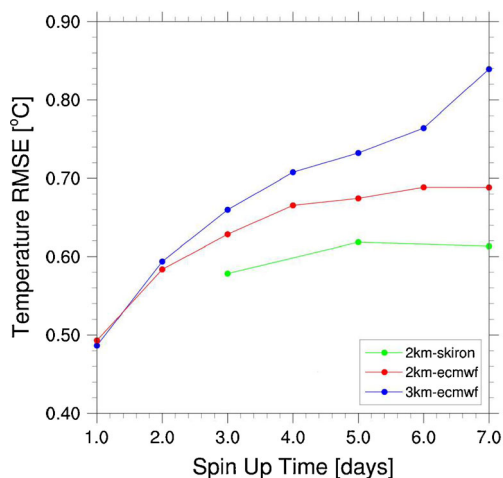


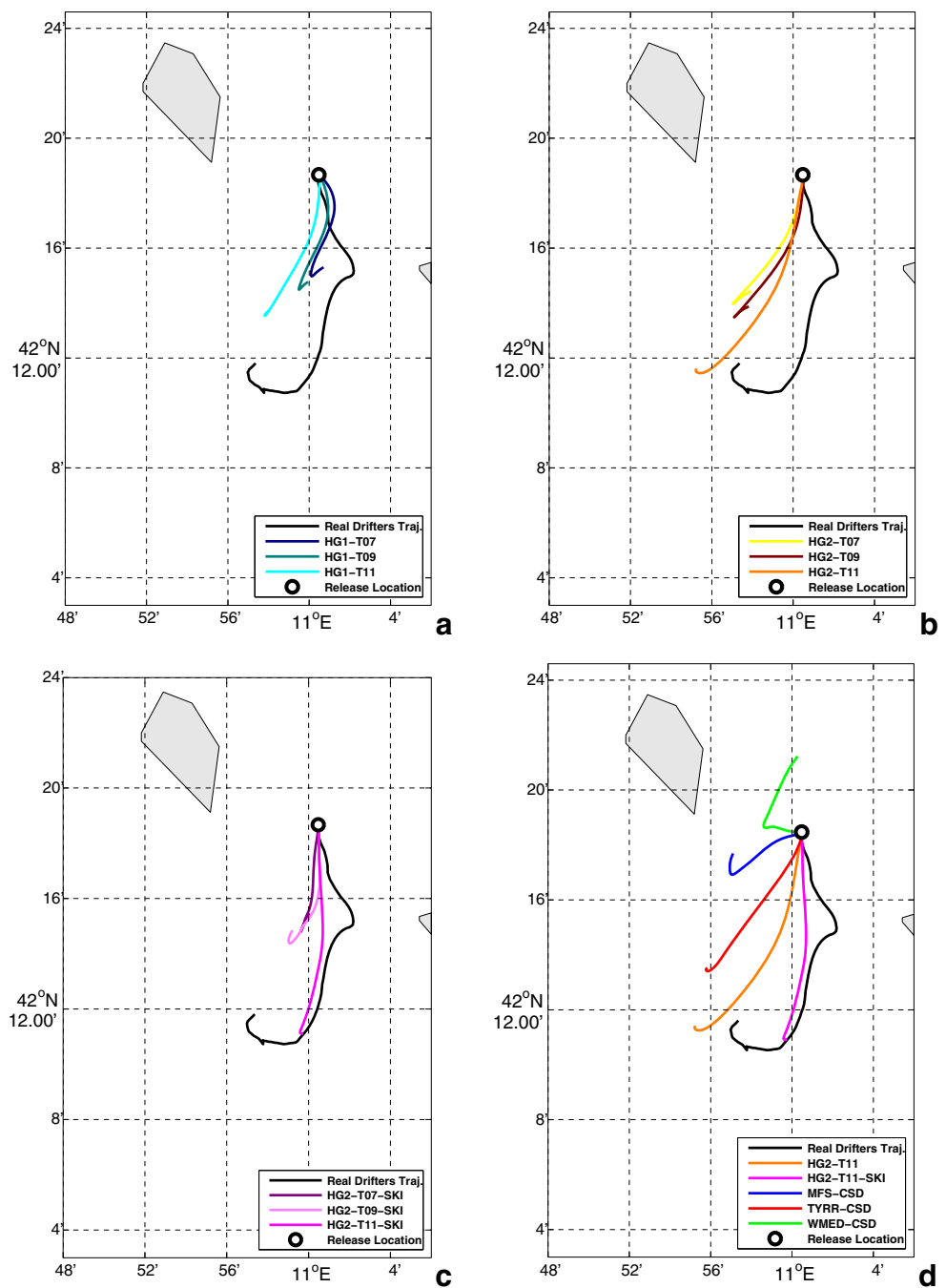
Fig. 10 Temperature RMSE calculated on day 14 February 12:00 UTC as function of spin-up time

shown (5 and 7 days spin-up time results are not shown). With this finer wind forcing, stronger westward currents develop south of the two islands, and the current between the Giglio and Giannutri Islands slightly changes its direction (eastward) compared to the currents presented in Fig. 8d, leading to better trajectories predictions (presented later in this section).

Furthermore, the model behavior related to initialization time and to the IRENOM and atmospheric model horizontal resolution is further investigated by comparing the model-predicted sea surface temperature (SST) to satellite radiometer observations available from the MyOcean portal (<http://www.myocean.eu/>) as daily gap-free map at 1/16° resolution over the Mediterranean Sea. Figure 10 shows the root mean square error (RMSE) statistics as a function of spin-up time for 3 and 2-km grid resolution. The HG2 configuration is in better agreement with observed SST, showing a lower RMSE than the HG1 configuration. For both model configurations, there is a progressive increase of RMSE as a function of spin-up time, suggesting that shorter spin-up time should lead to lower error in SST estimates. We have to consider that the father model (MFS) current fields are analysis, thus corrected using the assimilation of SST data. As a consequence, using a longer spin-up time, we let the IRENOM model free to develop its own dynamics, but possibly introducing a greater uncertainty when the model moves away from the MFS initial conditions, as confirmed by the trajectories predictions (presented later in this Section). As shown in Fig. 10, the IRENOM configuration with 2-km resolution and forced by the SKIRON 0.025° wind is in better agreement with the observed SST, showing a lower RMSE than the analogous configuration forced by the low-resolution ECMWF wind forcing.

The IRENOM configurations has been then validated using the trajectories of the drifters released in the Costa Concordia accident area. Figure 11a shows the trajectory prediction for buoy 1 using the IRENOM currents with resolution of 3 km and different spin-up times, forced by the ECMWF 0.25° wind forcing. The best result is achieved with the IRENOM currents initialized 3 days before the drifter deployment. Indeed, as shown in Table 5, Exp. HG1-T11 shows the lower separation distances and higher skill scores. Worse results are obtained increasing the spin-up time (Exp. HG1-T09 and Exp. HG1-T07), although little difference in trajectory prediction are observed using a spin-up time of 5 or 7 days. As depicted in Fig. 8a–c, a spin-up time longer than 3 days breaks the flow continuity that is observed along the channel. This fact causes a worst trajectory prediction for buoy 1, which follows a quite straight path across the channel. In summary, a greater spin-up time allows the generation of more spatial scales and stronger sea surface current, but it introduces uncertainties in the current fields when the model moves away from the MFS initial

Fig. 11 Simulated drifter trajectories using the IRENOM currents. **a** Horizontal resolution 3 km, with a spin-up time of 7 days (HG1-T07), 5 days (HG1-T09), and 3 days (HG1-T11). **b** Horizontal resolution of 2 km, with a spin-up time of 7 days (HG2-T07), 5 days (HG2-T09), and 3 days (HG2-T11). **c** Horizontal resolution of 2 km and SKIRON wind forcing (0.025°) with a spin-up time of 7 days (HG2-T07-SKI), 5 days (HG2-T09-SKI), and 3 days (HG2-T11-SKI). **d** Comparison between the simulated drifters obtained with the MFS, WMED, TYRR, and IRENOM currents with spin-up time (3 days), resolution 2 km, and ECMWF (HG2-T11) and SKIRON wind forcing (HG2-T11-SKI)



conditions, that is corrected using data assimilation. Moreover, in this specific case, longer spin-up time breaks the current which develops straight along the channel between the two islands, leading to a worst trajectory prediction for buoy 1.

Figure 11b shows the simulated trajectories using the IRENOM sea surface currents with a horizontal resolution of 2 km and spin-up time of 7, 5, and 3 days, forced by the ECMWF 0.25° wind forcing. The finer grid resolution allows the development of a stronger current in the channel. As a consequence, better trajectory prediction for

buoy 1 is achieved. The lowest separation distance after 24 h, 2.88 km, and a skill score of 0.75 is achieved using 3 days of spin-up and 2 km of resolution (Exp. HG2-T11, in Table 5). The spin-up time acts in the same way as for 3-km grid resolution. A 3-day spin-up time gives the best trajectory prediction, while longer spin-up times lead to a poorer trajectory prediction skill. In conclusion, it is suggested that the spin-up time for a relocatable model cannot be decided a priori and it should be a tuneable parameter.

Figure 11c shows the simulated trajectories using the IRENOM sea surface currents with a horizontal resolution

Table 5 Relocatable model performances in terms of trajectories separation distances and skill scores

Exp. name	Buoy1 d_{24h}	Buoy1 ss_{24h}	Mean d_{24h}	Mean ss_{24h}
HG1-T11	3.60 km	0.66	10.47 km	0.53
HG1-T09	6.39 km	0.57	11.56 km	0.48
HG1-T07	7.75 km	0.51	11.24 km	0.49
HG2-T11	2.88 km	0.75	10.06 km	0.59
HG2-T09	3.78 km	0.67	9.02 km	0.59
HG2-T07	4.78 km	0.62	8.87 km	0.58
HG2-T11-YS	2.87 km	0.74	10.15 km	0.58
HG2-T11-C5	3.16 km	0.75	10.21 km	0.57
HG2-T11-SKI	3.41 km	0.79	8.64 km	0.61
HG2-T09-SKI	5.96 km	0.59	7.82 km	0.56
HG2-T07-SKI	7.39 km	0.55	9.80 km	0.44

of 2 km and spin-up time of 7, 5, and 3 days, forced by the SKIRON 0.025° wind forcing. To be consistent with the IRENOM current fields, the Stokes drift correction, U_S of Eq. 7, and the wind drag correction, U_D of Eq. 5, are calculated by MEDSLIK-II using the SKIRON 0.025° wind

field. The finer wind forcing produces the change in the direction of the current in the channel, that is in this case more eastward directed, as shown in Fig. 8e. As a consequence, better trajectory prediction for buoy 1 is achieved. Although the separation distance after 24 h is 3.41 km (Exp.

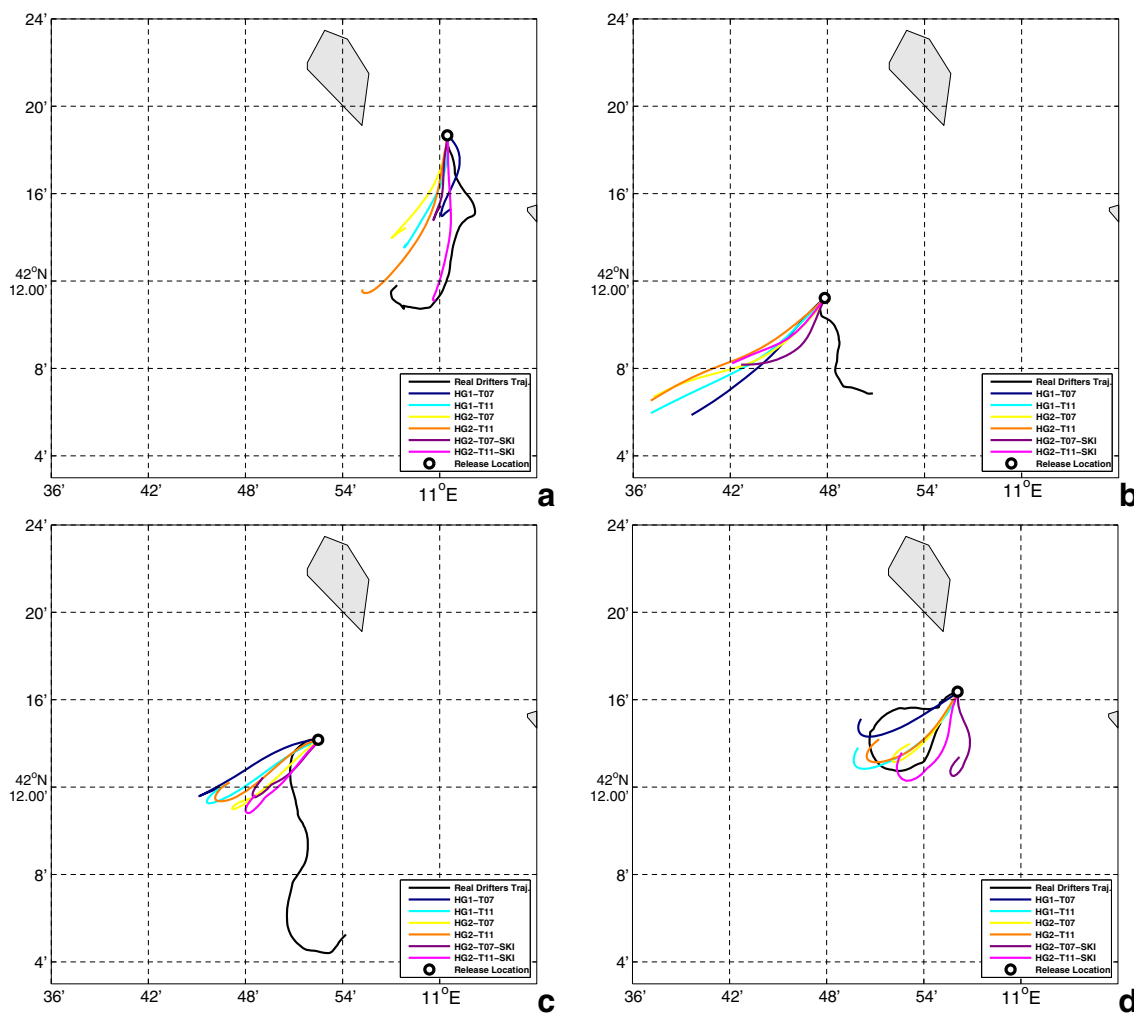


Fig. 12 Trajectory predictions using the different IRENOM models configurations: **a** buoy 1, **b** buoy 2, **c** buoy 3, and **d** buoy 4

HG2-T11-SKI, in Table 5), higher than in HG2-T11, it is qualitatively evident that the modeled trajectory using the high-resolution wind forcing is in better agreement with the observed trajectories. Indeed, Exp. HG2-T11-SKI shows the highest skill score (0.79) and in this case, as suggested by Liu and Weisberg (2011), the separation distance might not be a good estimate of the trajectory accuracy. In conclusion, higher resolution wind forcing gives a better estimate of the simulated drifter path.

Figure 11d shows the simulated trajectories using the MFS, TYRR, and WMED currents in comparison with the trajectories obtained with the IRENOM sea surface currents forced by both ECMWF 0.25° (HG2-T11) and SKIRON 0.025° (HG2-T11-SKI) with an horizontal resolution of 2 km, and spin-up time of 3 days, which are the best ones among the IRENOM experiments. The IRENOM currents give the best results. We believe this is due to the correct topography (Giglio and Giannutri Islands are correctly implemented in the model), and to the initialization procedure with a spin-up time of 3 days. In the MFS model, the Giglio Island is not reproduced, and although in WMED and TYRR model the Giglio Island is correctly defined, problems can arise from the initialization procedures: WMED has no spin-up time (cold start from MFS) and TYRR uses 7-days initialization period. Furthermore, the higher-resolution wind forcing further improves the modeled trajectories accuracy, while all the above operational models are forced by the ECMWF 0.25° forcing.

In Table 5, the skills of the trajectory simulations obtained using the IRENOM model with the Shapiro filter applied on the bathymetry for the configuration with 2-km grid resolution (HG2-T11-YS) and using a lower shallowest topography vertical clipping of 5-m value (HG2-T11-C5) with respect to the 10 m used for all the other experiments are shown. There is a meaningless difference in drifter trajectory predictions with respect to the case where the bathymetry is not filtered (HG2-T11). As well as using a lower shallowest topography clipping of 5-m value does not provide meaningful differences in skill trajectory predictions.

Figure 12 compares the trajectory predictions using the different IRENOM models configurations. Buoy 4 presents a looping behavior and the modeled trajectory is able to correctly reproduce the mean direction of the displacement, although it rotated in the opposite direction of the observed one. Moreover, it is evident that the trajectories of buoys 2 and 3 are not correctly reproduced. This might be due to the incorrect positioning of vortex structures that affects the buoys 2 and 3 movement. Indeed, as it is shown in the IRENOM HG2-T11-SKI model configuration vorticity section (Fig. 13), a baroclinic cyclonic vortex extends along the shelf. This vortex might be not correctly reproduced

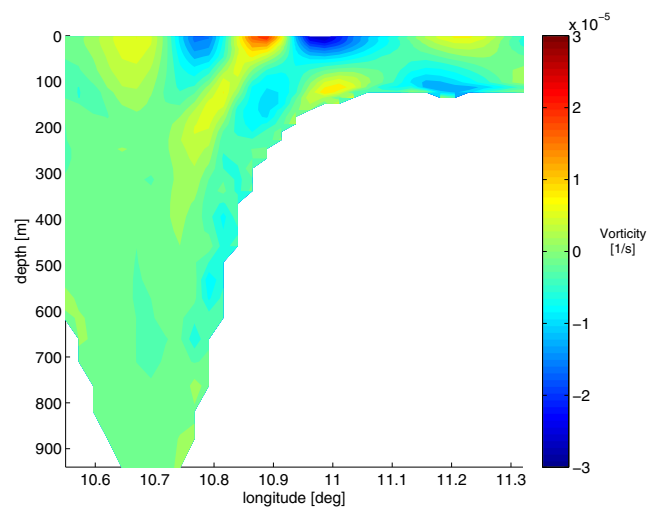


Fig. 13 Zonal vorticity section at 42°16' N of the IRENOM model with 2 km of resolution, 3 days of spin-up time, and forced by SKIRON 0.025° (HG2-T11-SKI). A baroclinic cyclonic vortex extends along the shelf

(misplaced or shifted in time) and negatively influences the trajectory predictions of buoys 2 and 3.

Besides the low performance of the IRENOM simulation in reproducing the buoys 2 and 3, the overall skill scores, listed in Table 5, confirm that the best configuration is the experiment HG2-T11-SKI with an overall skill score of 0.61. The mean separation distance appears to be lower in the HG2-T09-SKI, but as suggested by Liu and Weisberg (2011), the separation distance might not be a good estimate of the trajectory accuracy because looping trajectories may lead to an erroneous decrease of the separation distance, as it is the case of buoy 4.

5 Summary and conclusions

In this paper, the scientific tools that can be used to aid during an environmental emergencies are utilized and studied, including an evaluation of their performances. The paper presented step by step the improvements that are taken to produce better ocean state prediction. The final outcome is that high-resolution and accurate forecasts of the ocean currents that come from a relocatable ocean model (IRENOM) greatly improve the quality of the operational oceanography products: our best results showed that the skill score in trajectory predictions (and the separation distance) is 0.79 (3.41 km) using the IRENOM model, while using the coarser resolution model model it is 0.28 (11.05 km). Such forecasts and estimates can be given to the competent authorities during environmental emergencies.

First, we introduced the results of the operational support given during the Costa Concordia emergency. We found that a multimodel approach can show some degree of

confidence that any single model alone might not. When all the models are in agreement, we might be more confident in the accuracy of the forecasts. Despite being only qualitative comparison, a similar methodology was implemented during the Deepwater Horizon oil spill (Liu et al. 2011b, c) and it has demonstrated to provide some degree of confidence that any single model alone might not. One future solution would be to produce a unified daily product that could be easily used by all responders. We might expect that somehow combining models might improve the trajectory estimates. Few examples on using ocean ensembles in Lagrangian trajectory models are available (Vandenbulcke et al. 2009; Scott et al. 2012; Wei et al. 2013b). Those studies demonstrated that the ensemble can generate important uncertainty information, in addition to predicting the drifter trajectory with higher accuracy than a single ocean model forecast. More extensive new research on using ocean ensembles in Lagrangian trajectory predictions is expected in the near future.

Second, the deployment of drifters showed to be a key instrument to evaluate the models performance, as already demonstrated in other oil spill emergency cases (Caballero 2008; Liu and Weisberg 2011; Liu et al. 2011c; Mariano et al. 2011). The evaluation of the accuracy of the regional MFS model and subregional WMED and TYRR models is performed by using the drifters trajectory predicted by the oil spill model, MEDSLIK-II. This experiments allowed to calibrate the MEDSLIK-II trajectory model configuration, and we found that the best results are obtained using the Stokes drift and the wind drag correction. It has been found that the effect of wave and wind drag can be of the same order of magnitude of the currents velocity. We showed that using TYRR model with a resolution of 2 km, the lowest separation distance between modeled and observed trajectories is 4.15 km and the highest skill score is 0.59.

Third, we presented how a relocatable modeling methodology can improve the ocean state prediction accuracy. The IRENOM relocatable model has been nested in the MFS operational products and its performances have been evaluated using drifters trajectories. It has been shown that thanks to the possibility to change easily and quickly its configuration, the IRENOM results were of greater accuracy than the results achieved using regional (MFS) or subregional products (WMED and TYRR). We found that the reproduction of the correct topography, taking into account the small islands, that in a low-resolution model, such as MFS, are not correctly resolved, together with the initialization procedure are key configurations settings that should be correctly tuned. Regarding the initialization procedure, the general practice would suggest to choose the spin-up time which allows the ocean model to reach a state of physical equilibrium (Simoncelli et al. 2011). On the other

hand, as we found in this work, using a longer spin-up time, the IRENOM model is free to develop its own dynamics, but possibly introducing greater uncertainties when the model moves away from the MFS initial conditions (corrected using data assimilation). Thus, we can conclude that the spin-up time for a relocatable model cannot be decided a priori, but should be a tuneable parameter.

The best configurations of the IRENOM model are obtained using an initialization period of 3 days, a resolution of 2 km that allows the development of the stronger current in the channel between the two islands. Furthermore, the IRENOM currents forced by the wind forcing of SKIRON 0.025° better reproduced the current direction inside the channel. With this configuration (2 km, 3 days spin-up, SKIRON 0.025°), the skill score after 24 h of the MEDSLIK-II simulated trajectory for the buoy located in between the two island (buoy 1) is 0.79 and the separation distance is 3.41 km. On the other hand, with the same IRENOM configuration, two of the buoys were not correctly reproduced. This might be due to the incorrect positioning of vortex structures that affect the buoys movement. We believe that higher prediction skills might be achieved with increased resolution initial/boundary conditions or two-way-nesting to resolve smaller spatial scales. Besides this, the results are still in agreement with the state-of-the-art literature, showing an average separation distance after 24 h of 8.64 km, in agreement with the results found in the literature (Cucco et al. 2012; Huntley et al. 2011; Liu and Weisberg 2011; Röhrs et al. 2012), and the average skill score of 0.61.

Finally, we should remark that few data were available for the models validation during the Costa Concordia emergency case. A specific protocol to acquire data necessary for the models validation in a short time framework should be developed and employed. Rapid environmental assessment methodology for fast understanding of relevant environmental conditions at sea, in order to take tactical decisions, have been extensively developed in the past (Ferreira-Coelho and Rixen 2008) and should be now adapted to the specific scopes of environmental emergencies. Thus, in the future, we should design and validate an innovative methodology for response to oil spill events by using multiplatform observations (satellite, drifters, aerial surveys, and CTD surveys) to improve the models forecast skill. The final aim should be the rapid analysis of environmental and oil pollution conditions in order to set up a specific protocol for response to oil spill pollution at sea.

Acknowledgments This work has been funded by MEDESS4MS, TESSA and MyOcean2 Projects. We thank the Italian Coast Guard for the collaboration during the Costa Concordia emergency and the ARGOMARINE project for the drifters data.

Open Access This article is distributed under the terms of the Creative Commons Attribution License which permits any use, distribution, and reproduction in any medium, provided the original author(s) and the source are credited.

References

- Al-Rabeh AH, Lardner RW, Gunay N (2000) Gulfspill version 2.0: a software package for oil spills in the Arabian Gulf. *Environ Modell Softw* 15:425–442
- Agarwal A, Lermusiaux PFJ (2011) Statistical field estimation for complex coastal regions and archipelagos. *Ocean Model* 40(2):164–189
- Ambjörn C (2007) Seatrack web, forecasts of oil spills, a new version. *Environ Res Eng Manag* 3:60–66
- ASA (1997) OILMAP for Windows (technical manual). ASA Inc, Narrangansett
- ASCE (1996) State-of-the-art review of modeling transport and fate of oil spills. *J Hydraul Eng* 122:594–609
- Auclair F, Marsaleix P, Estournel C (2000) Sigma coordinate pressure gradient errors: evaluation and reduction by an inverse method. *J Atmos Ocean Technol* 17(10):1348–1367
- Barron CN, Smedstad LF, Dastugue JM, Smedstad OM (2007) Evaluation of ocean models using observed and simulated drifter trajectories: impact of sea surface height on synthetic profiles for data assimilation. *J Geophys Res* 112:C07019
- Bender MA, Ginis I, Tuleya R, Thomas B, Marchok T (2007) The operational GFDL coupled hurricane-ocean prediction system and a summary of its performance. *Mon Weather Rev* 135(12):3965–3989
- Berry A, Dabrowski T, Lyons K (2012) The oil spill model OILTRANS and its application to the Celtic Sea. *Mar Pollut Bull* 64:2489–2501
- Blain CA, Preller RH, Rivera AP (2002) Tidal prediction using the advanced circulation model (ADCIRC) and a relocatable PC-based system. *Oceanography* 15(1):77–87
- Blumberg A, Mellor G (1987) A description of a three-dimensional coastal ocean circulation model. In: Heaps NS (ed) Coastal estuarine science. American Geophysical Union, Three-dimensional Coastal Ocean Models, vol 116
- Caballero A, Espino M, Sagarminaga Y, Ferrer L, Uriarte A, González M (2008) Simulating the migration of drifters deployed in the Bay of Biscay, during the Prestige crisis. *Mar Pollut Bull* 56:475–482
- Carracedo P, Torres-López S, Barreiro M, Montero P, Balseiro CF, Penabad E, Leitao PC, Pérez-Muñuzuri V (2006) Improvement of pollutant drift forecast system applied to the Prestige oil spills in Galicia Coast (NW of Spain): development of an operational system. *Mar Pollut Bull* 53(5):350–360
- Castanedo S, Medina R, Losada IJ, Vidal C, Méndez FJ, Osorio A, Juanes JA, Puente A (2006) The Prestige oil spill in Cantabria Bay of Biscay. Part I: operational forecasting system for quick response, risk assessment, and protection of natural resources. *J Coast Res* 22:1474–1489
- Castellari S, Pinardi N, Leaman K (1998) A model study of air-sea interaction in the mediterranean sea. *J Mar Syst* 18:89–114
- Clementi E, Oddo P, Korres G, Drudi M, Pinardi N (2013) Coupled wave-ocean modelling system in the Mediterranean Sea. In: 13th international workshop on wave hindcasting and 4th coastal hazards symposium, Alberta
- Coppini G, De Dominicis M, Zodiatis G, Lardner R, Pinardi N, Santoleri R, Colella S, Bignami F, Hayes DR, Soloviev D, Georgiou G, Kallos G (2011) Hindcast of oil-spill pollution during the Lebanon crisis in the Eastern Mediterranean, July–August 2006. *Mar Pollut Bull* 62(1):140–153
- Cucco A, Sinerchia M, Ribotti A, Olita A, Fazioli L, Perilli A, Sorgente B, Borghini M, Schroeder K, Sorgente R (2012) A high-resolution real-time forecasting system for predicting the fate of oil spills in the Strait of Bonifacio (western Mediterranean Sea). *Mar Pollut Bull* 64(6):1186–1200
- Daniel P, Josse P, Dandin P, Gouriou V, Marchand M, Tiercelin C (2001) Forecasting the *Erika* oil spills. In: International oil spill conference, vol 2001, no 1, pp 649–655. American Petroleum Institute
- Daniel P, Marty F, Josse P, Skandrani C, Benschila R (2003) Improvement of drift calculation in Mothy operational oil spill prediction system. In: International oil spill conference (Vancouver, Canadian Coast Guard and Environment Canada), vol 6
- De Dominicis M, Leuzzi G, Monti P, Pinardi N, Poulain P (2012) Eddy diffusivity derived from drifter data for dispersion model applications. *Ocean Dyn* 62:1381–1398. doi:10.1007/s10236-012-0564-2
- De Dominicis M, Pinardi N, Zodiatis G, Lardner R (2013a) MEDSLIK-II, a Lagrangian marine surface oil spill model for short-term forecasting—part 1: theory. *Geosci Model Dev* 6:1851–1869. doi:10.5194/gmd-6-1851-2013
- De Dominicis M, Pinardi N, Zodiatis G, Archetti R (2013b) MEDSLIK-II, a Lagrangian marine surface oil spill model for short-term forecasting—part 2: numerical simulations and validations. *Geosci Model Dev* 6:1871–1888. doi:10.5194/gmd-6-1871-2013
- Debreu L, Blayo E (2008) Two-way embedding algorithms: a review. *Ocean Dyn* 58(5–6):415–428
- Dietrich DE, Ko DS, Yeske LA (1993) On the application and evaluation of the relocatable DieCAST ocean circulation model in coastal and semi-enclosed seas. Tech. Rep. 93-1, Center for Air Sea Technology, Mississippi State University, Stennis Space Center, MS
- Dietrich JC, Trahan CJ, Howard MT, Fleming JG, Weaver RJ, Tanaka S, Yuf L, Luettich RA Jr, Dawson CN, Westerink JJ, Wells G, Lu A, Vega K, Kubach A, Dresback KM, Kolar RL, Kaiser C, Twilley RR (2012) Surface trajectories of oil transport along the Northern Coastline of the Gulf of Mexico. *Cont Shelf Res* 41:17–47
- Dobricic S, Pinardi N (2008) An oceanographic three-dimensional variational data assimilation scheme. *Ocean Model* 22(3):89–105
- Ferreira-Coelho E, Rixen M (2008) Maritime rapid environmental assessment new trends in operational oceanography. *J Mar Syst* 69(12):1–2
- Gaberšek S, Sorgente R, Natale S, Ribotti A, Olita A, Astraldi M, Borghini M (2007) The sicily channel regional model forecasting system: initial boundary conditions sensitivity and case study evaluation. *Ocean Sci* 3:31–41
- Hackett B, Breivik Ø, Wettre C (2006) Forecasting the drift of objects and substances in the Ocean. *Ocean Weather Forecasting*. Springer, Netherlands, pp 507–523
- Haley Jr PJ, Lermusiaux PFJ (2010) Multiscale two-way embedding schemes for free-surface primitive-equations in the multidisciplinary simulation, estimation and assimilation system. *Ocean Dyn* 60:1497–1537
- Haley Jr PJ, Agarwal A, Lermusiaux PFJ (2013) Optimizing velocities and transports for complex coastal regions and archipelagos. *Ocean Model*, submitted
- Huntley HS, Lipphardt Jr BL, Kirwan Jr AD (2011) Lagrangian predictability assessed in the East China Sea. *Ocean Model* 36(1):163–178
- Isobe A, Hinata H, Kako S, Yoshioka S (2011) Formulation of leeway-drift velocities for sea-surface drifting-objects based on a wind-wave flume experiment. In: Omori K, Guo X, Yoshie N, Fujii

- N, Handoh IC, Isobe A, Tanabe S (eds) *Interdisciplinary studies on environmental chemistry-marine environmental modeling and analysis*. Terrapub., Tokyo, pp 239–249
- Jackson JB, Cubit JD, Keller BD, Batista V, Burns K, Caffey HM, Caldwell RL, Garrity SD, Getter CD, Gonzalez C, Guzman HM, Kaufmann KW, Knap AH, Levings SC, Marshall MJ, Steger R, Thompson RC, Weil E (1989) Ecological effects of a major oil spill on Panamanian coastal marine communities. *Science* 243(4887):37–44
- Janjic ZI (1984) Nonlinear advection schemes and energy cascade on semi-staggered grids. *Mon Weather Rev* 112:1234–1245
- Kallos G, Nickovic S, Jovic D, Kakaliagou O, Papadopoulos A, Misirlis N, Boukas L, Mimikou N (1997) The ETA model operational forecasting system and its parallel implementation. In: 1st workshop on large-scale scientific computations, Varna, Bulgaria, 7–11 June
- Kallos G, Papadopoulos A, Katsafados P, Nickovic S (2006) Transatlantic Saharan dust transport: model simulation and results. *J Geophys Res* 111:D09204
- Ko DS, Martin PJ, Rowley CD, Preller RH (2008) A real-time coastal ocean prediction experiment for MREA04. *J Mar Syst* 69(1):17–28
- Krishnamurti TN, Kishtawal CM, Zhang Z, LaRow T, Bachiochi D, Williford E (2000a) Multimodel ensemble forecasts for weather and seasonal climate. *J Clim* 13(23):4196–4216
- Krishnamurti TN, Kishtawal CM, Shin DW, Williford CE (2000b) Improving tropical precipitation forecasts from a multianalysis superensemble. *J Clim* 13(23):4217–4227
- Lardner R, Zodiatis G, Loizides L, Demetropoulos A (1998) An operational oil spill model for the Levantine Basin (Eastern Mediterranean Sea). In: International symposium on marine pollution
- Lardner R, Zodiatis G, Hayes D, Pinardi N (2006) Application of the MEDSLIK Oil spill model to the Lebanese Spill of July 2006. European group of experts on satellite monitoring of sea based oil pollution. European Communities
- Lehr W, Jones R, Evans M, Simecek-Beatty D, Overstreet R (2002) Revisions of the ADIOS oil spill model. *Environ Model Softw* 17:189–197
- Lermusiaux PFJ (1999) Estimation and study of mesoscale variability in the Strait of Sicily. *Dyn Atmos Oceans* 29:255–303
- Lermusiaux PFJ (2006) Uncertainty estimation and prediction for interdisciplinary ocean dynamics. Special issue of on uncertainty quantification. In: Glimm J, Karniadakis G (eds) Special issue of on uncertainty quantification, *Journal of Computational Physics*, vol 217, pp 176–199
- Lermusiaux PFJ (2007) Adaptive modeling, adaptive data assimilation and adaptive sampling. Special issue on Mathematical Issues and challenges in data assimilation for geophysical systems: interdisciplinary perspectives. In: Jones CKRT, Ide K (eds) Special issue on mathematical issues and challenges in data assimilation for geophysical systems: interdisciplinary perspectives. *Physica D*, vol 230, pp 172–196
- Lermusiaux PF, Haley Jr PJ, Yilmaz NK (2007) Environmental prediction, path planning and adaptive sampling-sensing and modeling for efficient ocean monitoring, management and pollution control. *Sea Technol* 48(9):35–38
- Lermusiaux PFJ, Haley Jr PJ, Leslie WG, Agarwal A, Logutov O, Burton LJ (2011) Multiscale physical and biological dynamics in the Philippines archipelago: predictions and processes. *Oceanography. PhilEx Issue* 24(1):70–89
- Leslie WG, Robinson AR, Haley Jr PJ, Logutov O, Moreno PA, Lermusiaux PFJ, Coelho E (2008) Verification and training of real-time forecasting of multi-scale ocean dynamics for maritime rapid environmental assessment. *J Mar Syst* 69(1):3–16
- Liu Y, Weisberg RH (2011) Evaluation of trajectory modeling in different dynamic regions using normalized cumulative Lagrangian separation. *J Geophys Res* 116:C09013
- Liu Y, MacFadyen A, Ji Z-G, Weisberg RH (2011a) Introduction to monitoring and modeling the deepwater horizon oil spill, in monitoring and modeling the deepwater horizon oil spill: a record-breaking enterprise. *Geophys Monogr Ser* 195: 1–7
- Liu Y, Weisberg RH, Hu C, Zheng L (2011b) Tracking the deepwater horizon oil spill: a modeling perspective. *Eos Trans AGU* 92(6):45–46
- Liu Y, Weisberg RH, Hu C, Zheng L (2011c) Trajectory forecast as a rapid response to the Deepwater Horizon oil monitoring and modeling the deepwater horizon oil spill: a record-breaking enterprise. *Geophys Monogr Ser* 195:153–165
- Logutov OG, Lermusiaux PFJ (2008) Inverse Barotropic tidal estimation for regional ocean applications. *Ocean Model* 25:17–34
- Lozano CJ, Robinson AR, Arango HG, Gangopadhyay A, Sloan Q, Haley PJ, Anderson L, Leslie W (1996) An interdisciplinary ocean prediction system: assimilation strategies and structured data models. *Elsevier Oceanogr Ser* 61:413–452
- Madec G (2008) NEMO ocean engine. Note du Pole de modélisation, Institut Pierre-Simon Laplace (IPSL), France, no 27, ISSN no 1288-1619
- Mariano A, Kourafalou V, Srinivasan A, Kang H, Halliwell G, Ryan E, Roffer M (2011) On the modeling of the 2010 Gulf of Mexico Oil Spill. *Dyn Atmos Oceans* 52:322–340. doi:10.1016/j.dynatmoce.2011.06.001
- Mason E, Molemaker J, Shchepetkin AF, Colas F, McWilliams JC, Sangrá P (2010) Procedures for offline grid nesting in regional ocean models. *Ocean Model* 35(1):1–15
- Mediterranean Forecasting System website: <http://gnoo.bo.ingv.it/mfs/myocean/>
- MEDSLIK-II website: <http://gnoo.bo.ingv.it/MEDSLIKII>
- Mellor GL (2004) User's guide for a three-dimensional, primitive equation numerical ocean model. International Report, Program in Atmospheric Ocean Science, Princeton University, Princeton, pp 11–35
- Mesinger F (1984) A blocking technique for representation of mountains in atmospheric models. *Riv Meteorol Aeronaut* 44:195–202
- MyOcean website: <http://www.myocean.eu/>
- Nittis K, Perivoliotis L, Korres G, Tziavos C, Thanos I (2006) Operational monitoring and forecasting for marine environmental applications in the Aegean Sea. *Environ Model Softw* 21:243–257
- Oddo P, Adani M, Pinardi N, Fratianni C, Tonani M, Pettenuzzo D (2009) A nested Atlantic-Mediterranean Sea general circulation model for operational forecasting. *Ocean Sci* 5(4):461
- Olita A, Ribotti A, Fazioli L, Perilli A, Sorgente R (2013) Surface circulation and upwelling in the western Sardinia sea: a numerical study. *Cont Shelf Res* 71:95–108
- Onken R, Robinson AR, Lermusiaux PFJ, Haley Jr PJ, Anderson LA (2002) Data-driven simulations of synoptic circulation and transports in the Tunisia-Sardinia-Sicily region. *J Geophys Res* 108(C9):8123–8136
- Onken R, Robinson AR, Kantha L, Lozano CJ, Haley PJ, Carniel S (2005) A rapid response nowcast/forecast system using multiply nested ocean models and distributed data systems. *J Mar Syst* 56(1):45–66
- Orlanski I (1976) A simple boundary condition for unbounded hyperbolic flows. *J Comput Phys* 21(3):251–269
- Peterson CH, Rice SD, Short JW, Esler D, Bodkin JL, Ballachey BE, Irons DB (2003) Long-term ecosystem response to the Exxon Valdez oil spill. *Science* 302(5653):2082–2086

- Platt JF, Anderson P (1996) Response of common murre to the Exxon Valdez oil spill and long-term changes in the Gulf of Alaska marine ecosystem. In: American fisheries society symposium, vol 18, pp 720–737
- Pinardi N, Coppini G (2010) Preface operational oceanography in the Mediterranean Sea: the second stage of development. *Ocean Sci* 6:263–267. doi:10.5194/os-6-263-2010
- Pollani A, Triantafyllou G, Petihakis G, Nittis K, Dounas C, Christoforos K (2001) The Poseidon operational tool for the prediction of floating pollutant transport. *Mar Pollut Bull* 43:270–278
- Posey PG, Allard RA, Preller RH, Dawson GM (2008) Validation of the global relocatable tide/surge model PCTides. *J Atmos Ocean Technol* 25(5):755–775
- Price JM, Reed M, Howard MK, Johnson WR, Ji ZG, Marshall CF, Guinasso NL, Rainey GB (2006) Preliminary assessment of an oil-spill trajectory model using satellite-tracked, oil-spill-simulating drifters. *Environ Model Softw* 21:258–270
- Proctor R, Elliot AJ, Flather RA (1994) Forecast and hindcast simulations of the Braer oil spill. *Mar Pollut Bull* 28(4):219–229
- Ramp SR, Lermusiaux PFJ, Shulman I, Chao Y, Wolf RE, Bahr FL (2011) Oceanographic and atmospheric conditions on the continental shelf north of the Monterey Bay during August 2006. *Dyn Atmos Oceans* 52:192–223
- Reed M, Gundlach E, Kana T (1989) A coastal zone oil spill model: development and sensitivity studies. *Oil Chem Pollut* 5:411–449
- Reed M, Turner C, Odulo A (1994) The role of wind and emulsification in modelling oil spill and surface drifter trajectories. *Spill Sci Technol B* 1:143–157
- Reed M, Aamo OM, Daling PS (1995) Quantitative analysis of alternate oil spill response strategies using OSCAR. *Spill Sci Technol Bull* 2:67–74
- Reed M., Johansen Ø, Brandvik PJ, Daling P, Lewis A, Fiocco R, Mackay D, Prentki R (1999) Oil spill modeling towards the close of the 20th century: overview of the state of the art. *Spill Sci Technol Bull* 5:3–16
- Rixen M, Ferreira-Coelho E (2007) Operational surface drift prediction using linear and non-linear hyper-ensemble statistics on atmospheric and ocean models. *J Mar Syst* 65(1):105–121
- Rixen M, Ferreira-Coelho E, Signell R (2008) Surface drift prediction in the Adriatic Sea using hyper-ensemble statistics on atmospheric, ocean and wave models: uncertainties and probability distribution areas. *J Mar Syst* 69(1):86–98
- Rixen M, Book J, Carta A, Grandi V, Gualdesi L, Stoner R, Ranelli P, Cavanna A, Zanasca P, Baldasserini G, Trangeled A, Lewis C, Trees C, Grasso R, Giannechini S, Fabiani A, Merani D, Berni A, Leonard M, Martin P, Rowley C, Hulbert M, Quaid A, Goode W, Preller R, Pinardi N, Oddo P, Guarnieri A, Chiggiato J, Carniel S, Russo A, Tudor M, Lenartz F, Vandenbulcke L (2009) Improved ocean prediction skill and reduced uncertainty in the coastal region from multi-model super-ensembles. *J Mar Syst* 78:S282–S289
- Robinson A (1999) Forecasting and simulating coastal ocean processes and variabilities with the Harvard Ocean Prediction System. Coastal Ocean Prediction, AGU Coastal and Estuarine Studies Series. *Am Geophys Union* 20:77–100
- Robinson AR, Sellschopp J (2002) Rapid assessment of the coastal ocean environment. In: Pinardi N, Woods JD (eds) Ocean forecasting: conceptual basis and applications. Springer, Berlin, pp 203–232
- Robinson AR, Arango HG, Miller AJ, Warn-Varnas A, Poulain PM, Leslie WG (1996) Real-time operational forecasting on shipboard of the Iceland-Faeroe frontal variability. *Bull Am Meteorol Soc* 72(2):243–259
- Robinson AR, Sellschopp J, Warn-Varnas A, Leslie WG, Lozano CJ, Haley Jr PJ, Anderson LA, Lermusiaux PFJ (1999) The Atlantic ionian stream. *J Mar Syst* 20:129–156
- Robinson AR, Haley PJ, Lermusiaux PFJ, Leslie WG (2002) Predictive skill, predictive capability and predictability in ocean forecasting. In: Proceedings of the The OCEANS 2002 MTS/IEEE conference. Holland Publications, pp 787–794
- Robinson AR, Sellschopp J, Leslie WG, Alvarez A, Baldasserini G, Haley Jr PJ, Lermusiaux PFJ, Lozano CJ, Nacini E, Onken R, Stoner R, Zanasca P (2003) Forecasting synoptic transients in the Eastern Ligurian Sea. In: Bovio E, Tyce R, Schmidt H (eds) Rapid environmental assessment. SACLANTCEN Conference proceedings series CP-46. Saclantcen, La Spezia
- Röhrs J, Christensen KH, Hole LR, Broström G, Drivdal M, Sundby S (2012) Observation-based evaluation of surface wave effects on currents and trajectory forecasts. *Ocean Dyn* 62(10–12):1519–1533
- Russo A, Coluccelli A (2006) Integration of a relocatable ocean model in the Mediterranean Forecasting System. *Ocean Sci Discuss* 3:1609–1621
- Schroeder AJ, Stauffer DR, Seaman NL, Deng A, Gibbs AM, Hunter GK, Young GS (2006) An automated high-resolution, rapidly relocatable meteorological nowcasting and prediction system. *Mon Weather Rev* 134(4):1237–1265
- Scott RB, Ferry N, Drévilion M, Barron CN, Jourdain NC, Lellouche JM, Metzger EJ, Rio M, Smedstad OM (2012) Estimates of surface drifter trajectories in the equatorial Atlantic: a multi-model ensemble approach. *Ocean Dyn* 62(7):1091–1109
- Simoncelli S, Pinardi N, Oddo P, Mariano AJ, Montanari G, Rinaldi A, Deserti M (2011) Coastal rapid environmental assessment in the Northern Adriatic Sea. *Dyn Atmos Oceans* 52(1):250–283
- Sorgente R, Drago AF, Ribotti A (2003) Seasonal variability in the central mediterranean sea circulation. *Ann Geophys* 21:299–322
- Sotillo M, Alvarez Fanjul E, Castanedo S, Abascal A, Menendez J, Emelianov M, Olivella R, García-Ladona E, Ruiz-Villarreal M, Conde J, Gómez M, Conde P, Gutierrez A, Medina R (2008) Towards an operational system for oil-spill forecast over Spanish waters: initial developments and implementation test. *Mar Pollut Bull* 56:686–703
- Spaulding M, Kolluru V, Anderson E, Howlett E (1994) Application of three-dimensional oil spill model (WOSM/OILMAP) to hindcast the Braer spill. *Spill Sci Technol Bull* 1:23–35
- Spyrou C, Mitsakou C, Kallos G, Louka P, Vlastou G (2010) An improved limited area model for describing the dust cycle in the atmosphere. *J Geophys Res* 115:D17211
- Thyrrhenian Forecasting system website: <http://utmea.enea.it/research/MEDMOD/>. Accessed 7 Feb 2014
- Tolman HL (2009) User manual and system documentation of WAVEWATCH III version 3.14. NOAA/NWS/NCEP/MMAB Tech. Note 276, 194 pp
- Tonani M, Pinardi N, Dobricic S, Pujol I, Fratianni C (2008) A high-resolution free-surface model of the Mediterranean Sea. *Ocean Sci* 4:1–14. doi:10.5194/os-4-1-2008
- Vandenbulcke L, Beckers JM, Lenartz F, Barth A, Poulain PM, Aidonidis M, Meyrat J, Arduin F, Tonani M, Fratianni C, Torrisi L, Pallela D, Chiggiato J, Tudor M, Book JW, Martin P, Peggion G, Rixen M (2009) Super-ensemble techniques: application to surface drift prediction. *Prog Oceanogr* 82(3):149–167
- Vetrano A, Napolitano E, Iacono R, Schroeder K, Gasparini GP (2010) Tyrrhenian Sea circulation and water mass fluxes in spring 2004: observations and model results. *J Geophys Res Oceans* 115(C6):C06023. doi:10.1029/2009JC005680
- Wang J, Shen Y (2010) Development of an integrated model system to simulate transport and fate of oil spills in seas. *Sci China Technol Sci* 53:2423–2434
- Wang S, Shen Y, Guo Y, Tang J (2008) Three-dimensional numerical simulation for transport of oil spills in seas. *Ocean Eng* 35:503–510

- Wei M, Jacobs G, Rowley C, Barron CN, Hogan P, Spence P, Smedstad OM, Martin P, Muscarella P, Coelho E (2013a) The impact of initial spread calibration on the RELO ensemble and its application to Lagrangian dynamics. *Nonlinear Process Geophys* 20:621–641
- Wei M, Jacobs G, Rowley C, Barron CN, Hogan P, Spence P, Smedstad OM, Martin P, Muscarella P, Coelho E (2013b) The performance of the US Navy's RELO ensemble, NCOM, HYCOM during the period of GLAD at-sea experiment in the Gulf of Mexico. *Deep Sea Research Part II: Topical Studies in Oceanography*
- Western Mediterranean Forecasting system website: <http://www.seaforecast.cnr.it/en/fl/wmed.php>
- Xie P, Arkin PA (1997) Global precipitation: a 17-year monthly analysis based on gauge observations, satellite estimates, and numerical model outputs. *Bull Am Meteorol Soc* 11:2539–2558
- Zelenke B, O'Connor C, Barker C, Beegle-Krause CJ, Eclipse L (eds) (2012) General NOAA Operational Modeling Environment (GNOME) Technical Documentation. U.S. Dept. of Commerce, NOAA Technical Memorandum NOS OR&R 40. Emergency Response Division, NOAA, Seattle, p 105, http://response.restoration.noaa.gov/gnome_manual